

1 **Uncertainty contributions to low-flow projections in Austria**

2

3 **J. Parajka¹, A.P. Blaschke¹, G. Blöschl¹, K. Haslinger², G. Hepp³, G., Laaha⁴, W.**
4 **Schöner⁵, H. Trautvetter³, A. Viglione¹ and M. Zessner³**

5 [1]{Institute for Hydraulic and Water Resources Engineering, TU Wien, Vienna, Austria}

6 [2]{Climate Research Department, Central Institute for Meteorology and Geodynamics,
7 Vienna, Austria}

8 [3]{Institute for Water Quality, Resource and Waste Management, TU Wien, Vienna,
9 Austria}

10 [4]{Institute of Applied Statistics and Computing, University of Natural Resources and Life
11 Sciences (BOKU), Vienna, Austria}

12 [5]{Department of Geography and Regional Science, University of Graz, Graz, Austria}

13 Correspondence to: J. Parajka (parajka@hydro.tuwien.ac.at)

14

15 **Abstract**

16 The main objective of the paper is to understand the contributions to the uncertainty in
17 low-flow projections resulting from hydrological model uncertainty and climate projection
18 uncertainty. Model uncertainty is quantified by different parameterizations of a conceptual
19 semi-distributed hydrologic model (TUWmodel) using 11 objective functions in three
20 different decades (1976-86, 1987-97, 1998-08), which allows disentangling the effect of the
21 objective function-related uncertainty and temporal stability of model parameters. Climate
22 projection uncertainty is quantified by four future climate scenarios (ECHAM5-A1B, A2, B1
23 and HADCM3-A1B) using a delta change approach. The approach is tested for 262 basins in
24 Austria.

25 The results indicate that the seasonality of the low-flow regime is an important factor
26 affecting the performance of model calibration in the reference period and the uncertainty of
27 Q_{95} low-flow projections in the future period. In Austria, the range of simulated Q_{95} in the
28 reference period is larger in basins with summer low-flow regime than in basins with winter

1 low-flow regime. The accuracy of simulated Q_{95} may result in a range of up to 60%
2 depending on the decade used for calibration.

3 The low-flow projections of Q_{95} show an increase of low flows in the Alps, typically in the
4 range of 10-30% and a decrease in the south-eastern part of Austria mostly in the range -5 to -
5 20% for the climate change projected for future period 2021-2050 relative the reference
6 period 1978-2007. The change in seasonality varies between scenarios, but there is a tendency
7 for earlier low flows in the Northern Alps and later low flows in Eastern Austria. The total
8 uncertainty of Q_{95} projections is the largest in basins with winter low-flow regime and, in
9 some basins the range of Q_{95} projections exceeds 60%. In basins with summer low flows, the
10 total uncertainty is mostly less than 20%. The ANOVA assessment of the relative contribution
11 of the three main variance components (i.e. climate scenario, decade used for model
12 calibration and calibration variant representing different objective function) to the low-flow
13 projection uncertainty shows that in basins with summer low-flows the climate scenarios
14 contribute more than 75% to the total projection uncertainty. In basins with winter low flow
15 regime, the median contribution of climate scenario, decade and objective function is 29%,
16 13% and 13%, respectively. The implications of the uncertainties identified in this paper for
17 water resources management are discussed.

18

19 **1 Introduction**

20 Understanding climate impacts on hydrologic water balance in general and extreme flows in
21 particular is one of the main scientific interests in hydrology. Stream flow estimation during
22 low-flow conditions is important also for a wide range of practical applications, including
23 estimation of environmental flows, effluent water quality, hydropower operations, water
24 supply or navigation. Projections of low flows in future climate conditions are thus essential
25 for planning and development of adaptation strategies in water resources management.
26 However it is rarely clear how the uncertainties in assumptions used in the projections
27 translate into uncertainty of estimated future low flows.

28 There are numerous regional and national studies that have analyzed the effects of climate
29 change on the stream flow regime, including low flows (e.g. Feyen and Dankers, 2009,
30 Prudhomme and Davies, 2009, Chauveau et al., 2013 among others). Most of them apply
31 outputs from different global or regional climate circulation models, which are based on
32 different emission scenarios. The projections of low flows are then typically simulated by

1 hydrologic models of various complexity. There is an increasing number of studies evaluating
2 different sources of uncertainty in river flow projections resulting from different GCMs,
3 downscaling methods or hydrologic model parametrization (e.g. Dobler et al., 2012, Finger et
4 al., 2012, Coron et al., 2012, Addor et al., 2014, Chiew et al., 2015). Only few studies,
5 however, evaluate the uncertainty of low-flow projections and the relative contribution of its
6 different sources (i.e. climate projection, hydrologic model structure and/or model
7 parameterizations). Such studies include assessment of the impact of different climate
8 projections on low flows evaluated e.g. in Huang et al. (2013) and Forzieri et al. (2014).
9 While Huang et al. (2013) assessed the low-flow changes and uncertainty in the five largest
10 river basins in Germany, Forzieri et al. (2014) evaluated the uncertainty of an ensemble of 12
11 bias corrected climate projections in the whole of Europe. Both studies quantified uncertainty
12 in terms of the number of low-flow projections that suggest the same change direction. Their
13 results indicated a consistent pattern of low-flow changes across different regions in Europe.
14 A common feature of such ensemble climate scenarios is an increase in the agreement
15 between ensemble members with increasing future time horizon of climate projections. The
16 impact of hydrologic model structure and climate projections was evaluated in Dams et al.
17 (2015). They applied four hydrologic models calibrated with four objective functions to
18 simulate the impact of three climate projections on low flows for a basin in Belgium. They
19 found that besides the uncertainty introduced by climate change scenarios, hydrologic model
20 selection introduces an additional considerable source of uncertainty in low-flow projections.
21 The model structure uncertainty was particularly important under more extreme climate
22 change scenarios. A similar study was performed by Najafi et al. (2011) who investigated the
23 uncertainty stemming from four hydrologic models calibrated by three objective functions
24 and applied on eight Global Climate Model (GCM) simulations in a basin in Oregon. Their
25 results showed that although in general the uncertainties from the hydrologic models are
26 smaller than from GCM, in the summer low-flow season, is the impact of hydrologic model
27 parametrization on overall uncertainty considerably larger than of the GCM.

28 The quantification of the relative contribution of different sources to the overall uncertainty of
29 stream flow projections is recently evaluated by using analyses of variance (ANOVA) (Storch
30 and Zwiers, 1999). Bosshard et al. (2013) synthetized previous studies that investigate
31 hydrological climate-impact projections and their sensitivity to different uncertainty sources.
32 They propose an ANOVA framework to separate the uncertainty from climate models,
33 statistical post-processing (bias correction and delta change approach) and hydrological

models. Addor et al. (2014) used the ANOVA framework to quantify the uncertainty of stream flow projections resulting from the combination of emission scenarios, regional climate models, post-processing methods, and hydrological models of different complexity. They reported that the main source of uncertainty stems from the climate models and natural climate variability, and the impact of emission scenario increases with increasing future time horizon of climate projections. Hingray and Said (2014) proposed a quasi-ergodic two-way ANOVA framework for the partitioning of the total uncertainty of climate projections. This framework is recently tested for the estimation of climate and hydrological uncertainties of transient low flow projections in two basins in the southern French Alps (Vidal et al., 2015). The results showed that a large part of the total uncertainty arises from the hydrological modelling and it can be even larger than the contribution from the GCMs.

The objective of this paper is to understand the relative contribution of the impact of hydrologic model calibration and ensemble climate scenarios to the overall uncertainty of low-flow projections in Austria. Here, the uncertainty and variability of low-flow projections is assessed for four climate scenarios, 11 variants of objective functions and three decades used for model calibration. Austria is chosen as a case study since it is an ideal test bed for such analysis, as it allows to disentangle the uncertainties separately in regions with summer and winter low-flow regimes. The assessment of uncertainties for winter and summer regimes allows to make generalisation for a similar spectrum of physiographic conditions around the world.

21

22 **2 Methodology**

23 **2.1 Low-flow projections**

In this study, low-flow projections of future climate scenarios are analysed by comparing future to past flows by using model forcing from a delta change approach. This concept allows to remove biases resulted from simulations when regional climate model (RCM) outputs are used as an input in hydrologic modelling. Instead of using RCM simulations of daily air temperature and precipitation for hydrologic model calibration, the model is first calibrated by using observed climate characteristics in the reference period. In a next step, RCM outputs are used to estimate monthly differences between simulations in the reference (control) and future periods. These differences (delta changes) are then added to the observed

1 model inputs and used for simulating future hydrologic changes. The daily precipitation is
 2 scaled by the relative monthly delta changes, with no change in the frequency of rainy days.
 3 The daily air temperature is changed by the absolute value of monthly delta changes. The
 4 differences between daily simulations of a hydrologic model in the reference and future
 5 periods are then used to interpret potential impacts of changing climate on future river flows.
 6 The future low-flow changes are quantified by the Q_{95} low-flow quantile and seasonality
 7 index SI . The Q_{95} represents river flow that is exceeded on 95% of the days of the entire
 8 reference or future period. This characteristic is one of the low-flow reference characteristic
 9 which is widely used in Europe (Laaha and Blöschl, 2006). Seasonality index SI represents
 10 the average timing of low flows within a year (Laaha and Blöschl, 2006, 2007). It is estimated
 11 from the Julian dates D_j of all days when river flows are equal or below Q_{95} in the reference
 12 or future periods. D_j represents a cyclic variable. Its directional angle, in radians, is given by:

$$13 \quad \theta_j = \frac{D_j \cdot 2\pi}{365} \quad (1)$$

14 The arithmetic mean of Cartesian coordinates x_θ and y_θ of a total of n single days j is defined
 15 as:

$$16 \quad x_\theta = \frac{1}{n} \sum_j \cos(\theta_j) \quad (2)$$

$$17 \quad y_\theta = \frac{1}{n} \sum_j \sin(\theta_j)$$

18 From this, the directional angle of the mean vector may be calculated by:

$$19 \quad \theta = \arctan\left(\frac{y_\theta}{x_\theta}\right) \quad \text{1st and 4th quadrant: } x > 0 \quad (3)$$

$$20 \quad \theta = \arctan\left(\frac{y_\theta}{x_\theta}\right) + \pi \quad \text{2nd and 3rd quadrant: } x < 0 \quad (4)$$

21 Finally, the mean day of occurrence is obtained from re-transformation to Julian Date:

$$22 \quad SI = \theta \cdot \frac{365}{2\pi} \quad (5)$$

23 and the variability of the date of occurrence about the mean date (i.e. seasonality strength) is
 24 characterized by the length parameter r . The parameter r is estimated as (Burn, 1997):

$$r = \sqrt{\bar{x}^2 + \bar{y}^2} / n \quad (6)$$

2 and ranges from $r=0$ (low strength, uniform distribution around the year) to $r=1$ (maximum
 3 strength, all extreme events of low flows occur on the same day).

The SI index is estimated for observed and simulated low flows. The differences between model simulations (i.e. Q_{95} and SI estimates) in the reference and future periods are then used to quantify potential impacts of climate change on low flows. Both Q_{95} and SI measures are estimated independently for the reference and future periods by the lfstat package in R software (Kofler and Laaha, 2014).

9

10 2.2 Hydrologic model

11 Low-flow projections are estimated by a conceptual semi-distributed rainfall-runoff model
12 (TUWmodel, Viglione and Parajka, 2014). The model simulates water balance components
13 on a daily time step by using precipitation, air temperature and potential evapotranspiration
14 data as an input. The model consists of three modules which allow simulating changes in
15 snow, soil storages and groundwater storages. The calibrated model parameters are presented
16 in Table 1. More details about the model structure and examples of application in the past are
17 given e.g. in Parajka et al. (2007, 2008), Viglione et al. (2013) and Ceola et al. (2015).

In this study, the TUWmodel is calibrated by using the SCE-UA automatic calibration procedure (Duan et al., 1992). The objective function (Z_Q) used in calibration is selected on the basis of prior analyses performed in different calibration studies in the study region (see e.g. Parajka and Blöschl, 2008, Merz et al., 2011). It consists of weighted average of two variants of Nash–Sutcliffe model efficiency, M_E and M_E^{log} . While the M_E efficiency emphasize the high flows, the M_E^{log} efficiency accentuates more the low flows. The maximized objective function Z_Q is defined then as

$$25 \quad Z_Q = w_Q \cdot M_E + (1 - w_Q) \cdot M_E^{\log} \quad (7)$$

where w_Q represents the weight on high or low flows. If w_Q equals 1 then the model is calibrated to high flows, if it equals to 0 then to low flows only. M_E and M_E^{log} are estimated as

$$1 \quad M_E = 1 - \frac{\sum_{i=1}^n (Q_{obs,i} - Q_{sim,i})^2}{\sum_{i=1}^n (Q_{obs,i} - \bar{Q}_{obs})^2} \quad (8)$$

$$2 \quad M_E^{\log} = 1 - \frac{\sum_{i=1}^n (\log(Q_{obs,i}) - \log(Q_{sim,i}))^2}{\sum_{i=1}^n (\log(Q_{obs,i}) - \bar{\log(Q_{obs}}))^2} \quad (9)$$

3 where $Q_{sim,i}$ is the simulated discharge on day i , $Q_{obs,i}$ is the observed discharge, \bar{Q}_{obs} is the
4 average of the observed discharge over the calibration (or verification) period of n days.

5

6 **2.3 Uncertainty estimation**

7 The uncertainty, defined as the range of simulated low-flow indices, is evaluated for two
8 contributions. The first analyses the uncertainty (i.e. the range of Q_{95} and SI) estimated for
9 different variants of hydrologic model calibration. Here, two cases are evaluated. In order to
10 assess the impact of time stability of model parameters (Merz et al., 2011), TUWmodel is
11 calibrated separately for three different decades (1976-1986, 1987-1997, 1998-2008). The
12 effect of objective functions used for the TUWmodel calibration is evaluated by comparing
13 11 variants of weights (w_Q) used in Z_Q . Following w_Q are tested: 0.0, 0.1, 0.2, 0.3, 0.4, 0.5,
14 0.6, 0.7, 0.8, 0.9 and 1.0. The hydrologic model is calibrated for all 11 variants in each
15 selected decade. Calibrated models are then used for flow simulations and hence Q_{95} and SI
16 estimation in the reference and future periods.

17 The second contribution evaluates the uncertainty of Q_{95} and SI changes simulated for
18 different climate scenarios. The effect of calibration uncertainty (case 1) is compared for four
19 selected climate scenarios (more details are given in Data section). The delta change approach
20 is used to derive model forcing for selected future period and simulated future river flows are
21 compared to model simulations in the reference period 1976-2008. The relative changes of
22 Q_{95} and SI values between reference and future periods are estimated for four selected climate
23 scenarios, 11 variants of model calibration and three selected decades. The relative
24 contribution of the impact of model calibration (i.e. time stability and objective function

1 selection) and climate scenario is evaluated for two low flow regimes and for individual
2 stations over Austria.

3 The uncertainty of low flow projections is then compared to the range of low-flow indices
4 obtained by different calibration variants in the reference period. In addition, the total
5 uncertainty of future low flow projections is decomposed to individual components by means
6 of analysis of variance (ANOVA; e.g. von Storch and Zwiers, 1999, chap. 9 for a general
7 introduction to ANOVA). The 3-way ANOVA approach is employed to decompose total
8 uncertainty of the projected low-flow changes into three main variance components. These
9 variance components represent uncertainty contributions of 3 main effects: climate scenario
10 (factor A with $I = 4$ levels), decade used for model calibration (factor B with $J = 3$, levels)
11 and calibration variant representing different objective functions (factor C with $K = 11$
12 levels). The ANOVA model is defined as follows:

13
$$\Delta Q95_{ijk} = \mu + \alpha_i + \beta_j + \gamma_k + \epsilon_{ijk} \quad (10)$$

14

15 In this linear equation (Eq.10), $\Delta Q95_{ijk}$ denotes the ensemble projected changes in Q_{95} for the
16 future horizon at a gauge. It is modelled by a global mean μ and the mean effects (deviations
17 of factor-means from the global mean) of climate scenario ($\alpha_i ; i = 1, \dots, I$), decade
18 ($\beta_j ; j = 1, \dots, J$), and calibration variant ($\gamma_k ; k = 1, \dots, K$), and ϵ_{ijk} are the residual errors of
19 the model. In an ANOVA framework, the total variance of $\Delta Q95_{ijk}$ is characterised by the
20 total sum of squares SS_T , and is decomposed into additive variance components of individual
21 effects:

22
$$S_T = SS_A + SS_B + SS_C + SS_E \quad (11)$$

23 The variance components of the main effects A, B, C are computed as follows:

1

$$SS_A = JK \sum_{i=1}^I (\bar{y}_{i..} - \bar{y}_{...})^2 \quad (12)$$

2

$$SS_B = IK \sum_{j=1}^J (\bar{y}_{.j.} - \bar{y}_{...})^2 \quad (13)$$

3

$$SS_C = IJ \sum_{k=1}^K (\bar{y}_{..k} - \bar{y}_{...})^2 \quad (14)$$

4

5 The variance component of the residuals representing the unexplained variance is:

6

$$SS_E = \sum_{i=1}^I \sum_{j=1}^J \sum_{k=1}^K (y_{ijk} - \bar{y}_{i..} - \bar{y}_{.j.} - \bar{y}_{..k} + \bar{y}_{...})^2 \quad (15)$$

7

8

9 Based on the SS_E , an estimate of the variance contributions of each effect A, B, C is computed
10 as:

11

$$\eta_A^2 = \frac{SS_A}{SS_T}; \quad \eta_B^2 = \frac{SS_B}{SS_T}; \quad \eta_C^2 = \frac{SS_C}{SS_T}; \quad \eta_E^2 = \frac{SS_E}{SS_T} \quad (16)$$

12

13 The measure eta-square is also termed the coefficient of determination R^2 (Von Storch and
14 Zwiers, 1999). Eta-square tends to overestimate the variance explained by one factor and is
15 therefore a biased estimate of the effect size. A less biased estimator is given by the measure
16 ω^2 :

17

$$\omega_A^2 = \frac{SS_A - df_A * MS_E}{SS_T - MS_E} \quad (17)$$

1 where df_A denotes the degrees of freedom of a factor (e.g. for factor A with I levels,
2 $df_A = I - 1$), and MS_E is the residual mean square error. Similar equations to Eq. 17 may be
3 written for factors B and C. The quantity MS_E denotes the mean residual sum of squares. It is
4 computed by

5
$$MS_E = \frac{SS_E}{df_E} \quad (18)$$

6
7 The measure omega-square is also termed the adjusted R^2 , in analogy to the adjusted
8 coefficient of determination of multiple regression. Note that the degrees of freedom of the
9 error term df_E depend on the total number of effects in the ANOVA design. For 3-way
10 ANOVA without interactions df_E is obtained by:

11
$$df_E = df_T - df_A - df_B - df_C = IJK - I - J - K + 2 \quad (19)$$

12 Clearly, the adjustment of effect size increases if the residual degrees of freedom are small,
13 what is the case when overall sample size is small. Hence the difference between both
14 measures of effect size will be negligible for designs with large df_E , as it is the case for our
15 study. In our assessment, we will therefore only present ω^2 which is the more general
16 measure of effect size at each catchment. A spatial synthesis of uncertainty contributions for
17 basins with summer and winter low-flow regime is finally obtained from the distribution of
18 variance components across basins falling into each low-flow regime group.

19

20 **3 Data**

21 Study region is Austria (Fig.1). Austria represents diverse climate and physiographic
22 conditions of Central Europe, which are reflected in different hydrologic regimes (Gaál et al.,
23 2012). The topography varies from 115 m a.s.l. in the lowlands to more than 3700 m a.s.l. in
24 the Alps. Austria is located in a temperate climate zone influenced by the Atlantic, meridional
25 south circulation and the continental weather systems of Europe. Mean annual air temperature
26 varies between -8°C to 10°C. The mean annual precipitation ranges from 550mm/year in the
27 Danube lowlands, to more than 3000mm/year on the windward slopes of the Alps.

1 The analysis is based on daily river flow measurements at 262 gauges (Fig. 1). This dataset
2 represents a subset of data used in Laaha and Blöschl (2006), which consists of gauges for
3 which hydrographs are not seriously affected by abstractions and karst effects during the low-
4 flow periods. Fig.1 shows two main low-flow regimes in Austria. While yellow circles
5 indicate 130 stations with dominant summer (June-November) low-flow occurrence, blue
6 circles indicates 132 gauges with winter (December-May) flow minima. These two groups
7 represent basins with distinct low-flow seasons, which are controlled by different hydrologic
8 processes. While the winter flow minima in the mountains are controlled by freezing
9 processes and snow storage, summer low flows occur during long-term persistent dry periods
10 when evapotranspiration exceeds precipitation. The different low-flow generating processes,
11 together with the hydro-climatic variety of the study area, gives rise to an enormous spatial
12 complexity of low flows in Austria. The largest values occur in the Alps, with typical values
13 ranging from 6 to $20 \text{ l s}^{-1} \text{ km}^{-2}$. The lowest values occur in the east ranging from 0.02 to 8 l s^{-1}
14 km^{-2} , although the spatial pattern is much more intricate.

15 Climate data used in hydrologic modeling consists of mean daily precipitation and air
16 temperature measurements at 1091 and 212 climate stations in the period 1976-2008,
17 respectively. Model inputs have been prepared by spatial interpolation and zonal averaging
18 described in detail in previous modeling studies (please see e.g. Merz et al., 2011 or Parajka et
19 al, 2007). These data serve as a basis for hydrologic model calibration and as a reference for
20 future change simulations. Fig. 2 shows basin averages of mean annual air temperature,
21 precipitation and runoff in the period 1976-2008. The two groups of basins (winter vs.
22 summer low flow regimes) clearly differ in the climate regime. Basins with summer low
23 flows are characterized by higher air temperatures, less precipitation and less runoff. The
24 comparison of three different decades indicates that mean annual air temperatures have
25 increased by 1°C in the period 1976-2008. This increase is similar for both groups of basins.
26 Interestingly, the mean annual precipitation has increased over the last three decades, which is
27 likely compensated by increased evapotranspiration, as the mean annual runoff remains rather
28 constant.

29 The regional climate model (RCM) scenarios used in this study are based on the results of the
30 reclip.century project (Loibl et al., 2011). The ensemble climate projections are represented
31 by COSMO-CLM RCM runs forced by the ECHAM5 and HADCM3 global circulation
32 models for three different IPCC emission scenarios (A1B, B1 and A2, Nakicenovic et al.,

1 2000). These represent a large spread of different emission pathways from a “business as
2 usual” scenario with prolonged greenhouse gas emissions (A2), a scenario with moderate
3 decline of emissions after 2050 (A1B) and a scenario indicating considerably reduced
4 emissions from now on (B1).

5

6 Table 2 summarizes the annual and seasonal differences (delta changes) of mean basin
7 precipitation and air temperature between the future (2021-2050) and reference (1978-2007)
8 periods. Table 2 indicates that the largest warming is obtained by simulations driven by
9 HADCM3. The median of air temperature increase in summer exceeds 2°C. In numerous
10 basins, a small decrease in air temperature in winter is simulated by ECHAM5 A2 and B1
11 simulations. The changes in mean annual precipitation are within the range ±9 % in all
12 selected basins. The increase tends to be larger in winter than in the summer period.

13

14 **4 Results**

15 **4.1 Low-flow simulations and uncertainty in the reference period**

16 The runoff model efficiency (Z_Q) in the three calibration periods obtained for different
17 variants of the objective function is presented in Fig. 3. The results show that Z_Q is larger and
18 thus runoff simulations are more accurate in basins with winter (blue colour) than summer
19 low-flow minimum (red colour). Most of the basins with winter low-flow regime are situated
20 in the alpine western and central part of Austria, where the runoff regime is snow dominated.
21 Such a regime has stronger runoff seasonality (see e.g. Fig. 5 in Laaha et al, this issue) and
22 less difference in rainfall regime, which allows to model rainfall–runoff process easier than in
23 basins with rainfall-dominated runoff regime. Z_Q increases with decreasing weight w_Q , which
24 indicates that the runoff model performance likely tends to be better for low than high flows.
25 The comparison of Z_Q in the three calibration periods indicates that the difference in model
26 performance between basins with winter and summer low-flow regime is the largest in the
27 period 1976-1986. While Z_Q for basins with winter low-flow regime is very similar in all
28 three calibration periods, Z_Q has an increasing tendency in basins with summer low-flow
29 regime. For example, the median of Z_Q for $w_Q=1.0$ increases from 0.64 in the period 1976-
30 1986 to 0.71 in the period 1998-2008. This increase is likely related to increasing number of
31 climate stations and data quality (Merz et al., 2009).

1 How the different calibration variants and periods translate into low-flow 95%- quantile Q_{95}
2 and seasonality SI is examined in Fig. 4. The model calibrated for 11 year period is used to
3 simulate daily flows in the entire reference period 1976-2008. The results show that the model
4 calibrated in the period 1976-1986 significantly overestimates Q_{95} of the reference period
5 particularly in basins with summer low-flow regime. The period 1976–1986 is characterized
6 by lower air temperatures with less evapotranspiration and relatively higher runoff generation
7 rates which translates into different soil moisture storage (FC model parameter) and runoff
8 generation (BETA) model parameters. Such effects are consistent with findings of Merz et al.,
9 (2011). The hydrologic model applied to the entire reference period hence produces larger
10 runoff contribution which tends to overestimate Q_{95} particularly in the warmer and drier parts
11 of the reference period and drier and warmer parts of Austria. The overestimation is consistent
12 for large range of w_Q (w_Q in the range 0.0-0.9) and the median of Q_{95} difference exceeds 20%.
13 Also the scatter around the median is rather large, where 25% of the basins with the summer
14 low-flow regime have Q_{95} differences larger than 35%. The simulated Q_{95} in basins with
15 winter low flows fit closer to the observed estimates. The median is less than 10% for variants
16 $w_Q < 1$. Interestingly, the model simulations based on calibration periods 1987-1997 and 1998-
17 2008 are much closer to the observed values. The results for both groups of basins are very
18 similar and essentially unbiased in terms of 95% low-flow quantile. The exception is the
19 calibration variant $w_Q=1$ that tends to underestimate Q_{95} . There are any significant differences
20 between calibration to low-flow only ($w_Q=0.0$) and other weights, with exception of $w_Q=1$,
21 which represents a typical calibration of using classical Nash-Sutcliffe coefficient.

22 The results of the seasonality estimation are presented in the bottom panels of Fig. 4. It is
23 clear that this hydrologic model tends to estimate the low-flow period later. This shift is larger
24 in basins with summer low-flow regimes. While the median of SI difference in basins with
25 winter low flows is around 10-12 days in the period 1976-1986 and increases to 12-19 days in
26 the period 1998-2008, the median of SI difference in basins with summer low flows is in the
27 range of 18-32 days. The scatter is, however, much larger for basins with summer low-flow
28 regime. Here the model simulates the season of low-flow occurrence with more than 2 months
29 shift (earlier or later) in almost 50% of the basins. A typical example of such shift is provided
30 in Fig. 5. The periods with flows below 95% quantile are often very short and the timing of
31 simulated low flows does not fit well with these periods. In some cases there is also a
32 difference in the length of observed and simulated low-flow periods. Some small rainfall-
33 runoff events in the summer or autumn cause an interruption of the observed low-flow

1 periods, but the model simulates a complete absorption of the precipitation event by the soil
2 storage and hence a longer low-flow period.

3 The spatial pattern of the variability of Q_{95} estimation in the reference period 1976-2008 is
4 presented in Fig. 6. Fig. 6 shows the range of differences between simulated and observed Q_{95}
5 for the different calibration variants. The results indicate that the Q_{95} differences vary more
6 between the different objective functions (right panels), however in many basins the range
7 exceeds 60% even if the model is calibrated by one objective function but in the different
8 calibration periods. As already indicated in Fig.4, the differences are larger in basins with
9 summer low flows, particularly for variants calibrated in the period 1976-1986. For particular
10 basins, the differences are not strongly related to the weight w_Q used in the calibration, with
11 an exception of $w_Q=1$, which tends to have the largest difference to observed Q_{95} . Some
12 examples of the model performance for individual basins are given in companion paper of
13 Laaha et al. (this issue).

14 Spatial variability of the model variability in terms of low-flow seasonality is presented in
15 Fig. 7. The results clearly indicate that basins with winter low-flow regime (i.e. situated in the
16 Alps) vary significantly less for different calibration settings than the basins with summer
17 low-flow regime. The range of differences is typically less than 14 days in the mountains,
18 compared to more than 90 days in many basins with the summer low-flow regime.

19 The comparison of SI and Q_{95} ranges indicates that large SI variability does not systematically
20 mean large variability in terms of Q_{95} . For example, a cluster of basins situated in the south-
21 eastern part of Austria (Styria) has a large SI range of difference (i.e. more than 90 days) for
22 11 calibration variants in the period 1976-1986, but the variability in Q_{95} is in many basins
23 less than 20% for this case. The same applies for the opposite case of small SI and large Q_{95}
24 variability in the alpine basins.

25

26 **4.2 Low-flow projections and uncertainty in the future period**

27 Low-flow projections for selected climate scenarios and different calibration weights w_Q are
28 presented in Fig. 8. Rather than to evaluate in detail the projections in terms of absolute
29 values of low-flow changes, the main focus is to assess the range of possible changes caused
30 by different scenarios and objective function used for model calibration. The results show
31 projections based on model calibration in 1998-2008, but the results are almost identical with

1 results for the other two calibration periods (i.e. the average difference is around 1%). Fig. 8
2 clearly shows the difference in projections for basins with summer and winter low-flow
3 regime, particularly for Q_{95} changes. It is hence important to evaluate the projections and their
4 variability separately for different regimes. The comparison of different scenarios indicates
5 that they are similar in terms of projecting an increase of winter low flows and a tendency for
6 no change or decreasing low flows in the summer period. The increase of winter Q_{95} slightly
7 varies between climate scenarios and tends to increase for calibration variants with larger w_Q .
8 The difference in median between $w_Q < 0.4$ and $w_Q > 0.8$ is approximately 9%. The projections
9 of Q_{95} changes in basins with summer low flows have significantly smaller variability and do
10 not depend on w_Q . The change in low-flow seasonality (Fig. 8, bottom panels) is less
11 pronounced. The median of projections is around 5 and 10 days earlier than in the reference
12 period for basins with summer and winter low-flow regime, respectively. Interestingly, the
13 variability between basins and w_Q is significantly smaller than obtained for different
14 calibration variants in the reference period (Fig. 4).

15 Examples of spatial patterns of low-flow projections are presented in Fig. 9 and 10. The
16 projections of Q_{95} changes (Fig. 9) indicate an increase of low flows in the Alps, typically in
17 the range of 10-30%. A decrease is simulated in south-eastern part of Austria (Styria) mostly
18 in the range of -5 - -20%. The most spatially different projection is provided by the HADCM3
19 A1B climate scenario which simulates the strongest gradient between an increase of Q_{95} in the
20 Alps in winter and a decrease in south-eastern part in summer. The change in the seasonality
21 varies between the scenarios, but there is a tendency for earlier low flows in the Northern
22 Alps and a shift to later occurrence of low flows in the Eastern Austria (Fig. 10). As already
23 indicated in Fig. 8, the shift in seasonality is larger than one month only in a few basins.

24 Figure 9 and 10 show projections of low flows for four climate scenarios, but only one set of
25 hydrologic model parameters. The evaluation of the impacts of different calibration variants
26 on the variability of low-flow projections is presented in Fig. 11 and 12. These figures
27 indicate the range of Q_{95} (Fig. 11) and the seasonality occurrence (Fig. 12) changes obtained
28 by 11 calibration variants and three calibration periods. The range of Q_{95} changes is
29 interestingly the largest in basins with the winter low-flow regime. In the Alps, the increase of
30 Q_{95} is often in the range of 15% to more than 60%. On the other hand, the future Q_{95}
31 estimates vary only slightly between the calibration variants in basins with the summer low
32 flows. The change is less than 20% in most of the basins. The impact of the selection of

1 objective function is, however, much larger for the estimation of the seasonality changes.
2 Depending on the calibration variant, the change in seasonality can vary within more than 3
3 months, e.g. in the south-eastern part of Austria.

4 The total uncertainty of low-flow projections of Q_{95} and SI is presented in Fig. 13. While the
5 top panels show the range of low-flow characteristics for all climate scenarios, calibration
6 variants and periods, the bottom panels show the ratio between the uncertainty of future
7 low-flow projections to the range of low-flow indices simulated in the reference period. The
8 results show that the Q_{95} range is less than 25% in approximately one third of analyzed
9 basins. On the other hand, 20% of basins have a range larger than 50%. These are the basins
10 with the winter low-flow regime. The variability in the date of low-flow occurrence is less
11 than three months in 40% of the basins. In almost 20% of the basins, however, it is larger than
12 five months. The ratio between the range of projections to the range of calibration differences
13 (bottom panels in Fig. 13 and Fig. 14) indicates that only in 15% of the cases the climate
14 projection uncertainty of Q_{95} is larger than the range obtained in the calibration period. Most
15 of these basins are situated in the mountains (mean basin elevation above 1000m a.s.l.) and
16 have winter low-flow regime. The range of calibrated Q_{95} is larger in almost all basins with
17 the summer low-flow regime, which are characterized by lower mean basin elevation and
18 larger aridity (i.e. ratio of mean annual potential evaporation to mean annual precipitation).
19 On the other hand, the climate projection uncertainty dominates for the low-flow seasonality
20 and is more than three times larger in 50% of basins, particularly in the Alps. The SI
21 projection uncertainty is only in 15% of the basins lower than the SI range obtained in the
22 calibration period. The SI uncertainty ratio tends to be lower with increasing mean basin
23 elevation and the basin area, but there is no apparent relationship with the aridity of the
24 basins.

25 The relative contribution of the three main variance components (i.e. climate scenario, decade
26 used for model calibration and calibration variant representing different objective function) to
27 the overall uncertainty of future low-flow projections is evaluated in Fig. 15. Left and right
28 panels show the distribution of ANOVA variance components for basins with winter (left
29 panel) and summer (right panel) low-flow regime, respectively. The results indicate that the
30 variability from climate scenarios has a dominant contribution to the overall projection
31 uncertainty in basins with summer low-flow regime. While in basins with winter low flows
32 the median contribution of the three variance components is 29% (climate scenario), 13%

1 (calibration decade) and 13% (objective function), in basins with summer low-flow regime is
2 the median contribution from climate scenario larger than 76%.

3

4 **5 Discussion and conclusions**

5 The objective of the study is to explore the relative role of hydrologic model calibration and
6 climate scenarios in the uncertainty of low-flow projections. While many previous studies
7 simulate only the change in hydrologic regime or extreme characteristics due to changes in
8 climate, in this study we focus on the quantification of the range of low-flow projections (i.e.
9 uncertainty) due to differences in the objective function used in model calibration, temporal
10 stability of model parameters and an ensemble of climate projections.

11 There are a number of studies that compare the uncertainty of projected runoff changes due to
12 different model structure, objective function or GCM and emission scenarios. These studies
13 found that the hydrologic model uncertainty tends to be considerably smaller than that from
14 GCM or emission scenarios (Najafi et al., 2011, Prudhomme and Davies, 2009). Such results,
15 however, refer to the seasonal or monthly runoff and are based on only a limited number of
16 basins. The quantification of the uncertainty in low flows is still rather rare. Some studies
17 (e.g. Huang et al., 2013 and Forzieri et al., 2014) evaluate the low-flow uncertainty in terms
18 of the number of projections with the same change direction. They showed that the
19 uncertainty is controlled mainly by the differences in emission scenarios and it decreases with
20 increasing projection horizon. Our results indicate that, although the uncertainty from
21 different climate scenarios is larger than 40% in many basins, the range of low-flow indices
22 from model calibration can exceed 60%. This result particularly relates to the assessment of
23 low-flow quantile changes.

24 Some recent low-flow studies suggest to more explicitly distinguish between the processes
25 leading to low-flow situations (see e.g. Fleig et al., 2006, Laaha et al., 2006, Van Loon et al.,
26 2015, Forzieri et al., 2014). Following this recommendation, we analyzed the effects of model
27 calibration and climate scenarios separately for basins with dominant winter and summer low-
28 flow regimes. Our results indicate that the calibration runoff efficiency in basins with winter
29 low-flow regime is larger (more accurate), and varies between basins less than in basins with
30 summer low-flow regime. The calibration uncertainty in basins with summer low flows
31 exceeds in many basins 60% even if the model is calibrated by the same objective function
32 but in different calibration periods. This finding confirms and quantifies the potential impact

of time stability of model parameters reported by Merz et al. (2011). The model parameters calibrated in colder periods with relatively larger runoff generation rates tend to overestimate low flows, particularly in basins with summer low-flow regime and in warmer and drier parts of the simulation period. The results indicate that the time stability of model parameters is not sensitive to the weighting of normal (M_E) and logarithmic transformed (M_E^{log}) Nash-Sutcliffe efficiency in the objective function used for calibration. The exception is the case of using only M_E with no weight on M_E^{log} , which does not allow accurate low-flow simulations. This finding partly supports the studies that propose logarithmically transformed discharge values for calibrating hydrologic models with a focus on low flows (please see review in Pushpalatha et al., 2012). Our results show that the impact of the objective function is larger for SI estimation in basins with summer low-flow regime in the reference period and for future projections of Q_{95} in basins with winter low-flow regime. Depending on the calibration variant, the change in seasonality can vary within more than three months, which clearly indicates a shift in the main hydrologic processes causing the low flows.

The climate change signals captured in selected scenarios are well within the range of the projections of the ENSEMBLES regional climate simulations for Europe (van der Linden and Mitchell, 2009; Heinrich and Gobiet, 2011). Jacob et al. (2015) showed that the most recent regional climate simulations over Europe, accomplished by the EURO-CORDEX initiative (RCPs, Moss et al., 2010), are rather similar to the older ENSEMBLES simulations with respect to the climate change signal and the spatial patterns of change. Although this ensemble of four scenario runs seems rather small, the selection accomplished by the reclip:century consortium was not arbitrary, but based on quantitative metrics. Prein et al. (2011) investigated the performance of all GCMs in CMIP3 for Central Europe based on a performance index including various parameters. They found that for the given domain the ECHAM5 and the HADCM3 showed highest scores, which justified the selection of these GCMs for driving the RCM. In addition, these two models show different climate sensitivity, where the warming over the course of the 21st century is lower in ECHAM5 and higher in HADCM3. This feature in combination with the utilization of three different scenarios for ECHAM5 provides broad ensemble bounds, although the climate change signal of the different scenarios for the given investigation period (2021-2050) is rather similar, particularly for air temperature (cf. Table 1). The projected future decrease of Q_{95} is most pronounced in the AIT_HADCM3_A1B run, particularly in basins with summer low-flow regime in the low lands. As indicated in Heinrich and Gobiet (2011), the climate sensitivity of

1 HADCM3 is higher than that of ECHAM5, which translates into a higher warming rate of 2.1
2 °C in summer (c.f. Table 1) compared to 1.2 °C in the ECHAM5 driven run. The higher
3 evaporative demand due to the increased air temperature signal translates into the strongest
4 change of the summer low-flow signal.

5 The comparison of the ranges of low-flow indices projected for different climate scenarios
6 and simulated by different calibration settings (i.e. objective function and calibration decade)
7 in the reference period indicates that the variability of low-flow magnitudes is larger for
8 simulations in the reference period, while the range of seasonality is larger for future
9 projections. Previous ENSEMBLES and CORDEX studies showed that RCM uncertainty is
10 far from being negligible for hydrology-related variables. Even if only one RCM is tested
11 here and the variability and uncertainty of GCM and emission scenarios can be large, the
12 results clearly indicate the importance of selecting objective functions in hydrologic model
13 calibration for simulating low-flow projections.

14 In our study, we use a 3-way ANOVA approach to decompose the contribution of climate
15 scenarios and hydrologic model settings to the total uncertainty of low-flow projections.
16 While previous studies (e.g. Hingray and Said 2014; Lafaysse et al., 2014, Vidal et al, 2015)
17 assessed the variance components of a temporal change from the multi-member ensemble
18 runs in individual basins, in our study, we lumped the temporal change to one time slice
19 (future horizon) and assessed the variance components in a spatial context of 262 basins. The
20 spatial synthesis of the uncertainty contribution is evaluated for two groups of basins,
21 representing to main (summer and winter) low-flow regimes in Austria. We found that the
22 relative contribution of three variance components - climate scenarios, calibration decade and
23 calibration objective function differs for basins with different low-flow regimes. The
24 uncertainty from climate scenarios dominates in basins with summer low flows, however in
25 basins with winter low flows is the relative contribution from hydrological modelling
26 significantly larger. This is consistent with previous studies that show a substantial
27 uncertainty contribution of hydrological models in basins dominated by snow and ice melt
28 (Addor et al.,2014, Vidal et al., 2015).

29 The assessment in Austria enabled us to account for one conceptual hydrologic model and
30 two different low-flow regimes. In the future we plan to extend such comparative assessment
31 to more types of low flows (e.g. as classified in Van Loon and Van Lanen, 2012), their
32 combinations linked with changes in land use and management at the wider, European scale,

1 as well as to account for hydrologic models of different complexity, wider range of climate
2 scenarios and different downscaling techniques. This will allow us to shed more light on the
3 factors controlling the possible scenarios of low-flow and water resources changes in the
4 future.

5 From the practical point of view, the projections of Q_{95} changes and related uncertainties are
6 an essential input to water quality modelling. The exceedance of environmental quality
7 standards (BGBI II Nr. 99/2010; Zessner, 2008) in case of emissions from point sources (e.g.
8 waste water treatment plants) increases the vulnerability of water resources, particularly
9 during low-flow conditions. We therefore also plan to evaluate the impact of climate
10 projection and hydrologic model uncertainties on the assessment of water quality and its
11 changes.

12

13 **Acknowledgements**

14 We would like to thank the Austrian Climate and Energy Fund (Project B060362-CILFAD,
15 Project Nr KR13AC6K11034-AQUASTRESS) for financial support. At the same time, we
16 would like to thank the Hydrographical Service of Austria (HZB) and the Central Institute for
17 Meteorology and Geodynamics (ZAMG) for providing hydrologic and climate data.

18

1 **References**

- 2 Addor, N., Rössler, O., Köplin, N., Huss, M., Weingartner, R., and Seibert, J.: Robust
3 changes and sources of uncertainty in the projected hydrological regimes of Swiss
4 catchments, *Water Resour. Res.*, 50, 7541–7562, doi:10.1002/2014WR015549, 2014.
- 5 BGBI II Nr. 99/2010: Bundesgesetzblatt für die Republik Österreich, Qualitätszielverordnung
6 Ökologie Oberflächengewässer – QZV Ökologie OG, Jahrgang 2010.
- 7 Bosshard, T., Carambia, M., Goergen, K., Kotlarski, S., Krahe, P., Zappa, M., and Schär, C.:
8 Quantifying uncertainty sources in an ensemble of hydrological climate-impact projections,
9 *Water Resour. Res.*, 49, 1523–1536, doi:10.1029/2011WR011533, 2013.
- 10 Ceola, S., Arheimer, B., Baratti, E., Blöschl, G., Capell, R., Castellarin, A., Freer, J., Han, D.,
11 Hrachowitz, M., Hundecha, Y., Hutton, C., Lindström, G., Montanari, A., Nijzink, R.,
12 Parajka, J., Toth, E., Viglione, A., and Wagener, T.: Virtual laboratories: new opportunities
13 for collaborative water science, *Hydrol. Earth Syst. Sci.*, 19, 2101-2117, doi:10.5194/hess-19-
14 2101-2015, 2015.
- 15 Coron L., Andréassian V., Perrin C., Lerat J., Vaze J., Bourqui M., and Hendrickx F.: Crash
16 testing hydrological models in contrasted climate conditions: An experiment on 216
17 Australian catchments, *Water Resources Research*, 48 (5), doi: 10.1029/2011WR011721,
18 2012.
- 19 Dams, J., Nossent, J., Senbeta, T.B., Willems, P., and Batelaan, O.: Multi-model approach to
20 assess the impact of climate change on runoff, *Journal of Hydrology*, 529(3), 1601–1616
21 doi:10.1016/j.jhydrol.2015.08.023, 2015.
- 22 Dobler, C., Hagemann, S., Wilby, R. L., and Stötter, J.: Quantifying different sources of
23 uncertainty in hydrological projections in an Alpine watershed, *Hydrol. Earth Syst. Sci.*, 16,
24 4343–4360, doi:10.5194/hess-16-4343-2012, 2012.
- 25 Duan, Q., Sorooshian, S., and Gupta, V.K.: Effective and efficient global optimization for
26 conceptual rainfall-runoff models, *Water Resources Research*, 28, 1015–1031, 1992.
- 27 Feyen, L., and Dankers, R.: Impact of global warming on streamflow drought in Europe, *J.*
28 *Geophys. Res.*, 114, D17116, doi:10.1029/2008JD011438, 2009.
- 29 Finger, D., Heinrich, G., Gobiet, A., and Bauder, A.: Projections of future water resources and
30 their uncertainty in a glacierized catchment in the Swiss Alps and the subsequent effects on

- 1 hydropower production during the 21st century, Water Resour. Res., 48, W02521,
2 doi:10.1029/2011WR010733, 2012.
- 3 Fleig, A.K., Tallaksen, L.M., Hisdal, H., and Demuth, S.: A global evaluation of streamflow
4 drought characteristics, Hydrol. Earth Syst. Sci., 10, 535–552, 2006.
- 5 Forzieri, G., Feyen, L., Rojas, R., Flörke, M., Wimmer, F., and Bianchi, A.: Ensemble
6 projections of future streamflow droughts in Europe, Hydrol. Earth Syst. Sci., 18, 85–108,
7 doi: 10.5194/hess-18-85-2014, 2014.
- 8 Gaál, L., Szolgay, J., Kohnová, S., Parajka, J., Merz, R., Viglione, A., and Blöschl, G.: Flood
9 timescales: Understanding the interplay of climate and catchment processes through
10 comparative hydrology, Water Resources Research, 48(4), W04511, doi:
11 10.1029/2011WR011509, 2012.
- 12 Hingray, B., and Said, M.: Partitioning internal variability and model uncertainty components
13 in a multimember multimodel ensemble of climate projections, Journal of Climate, 27, 17,
14 6779, doi: <http://dx.doi.org/10.1175/JCLI-D-13-00629.1>, 2014.
- 15 Huang, S., Krysanova, V., and Hattermann, F. F.: Projection of low flow conditions in
16 Germany under climate change by combining three RCMs and a regional hydrological model,
17 Acta Geophysica, 61 (1), 151-193, 2013.
- 18 Chauveau, M., Chazot, S., Perrin, C., Bourgin, P., Sauquet, E., Vidal, J., Rouchy, N., Martin,
19 E., David, J., Norotte, T., Maugis, P., and de Lacaze, X.: What impacts of climate change on
20 surface hydrology in France by 2070?, La Houille Blanche, (4), 5-15, 2013.
- 21 Chiew, F. H. S., Zheng, H., and Vaze, J.: Implication of calibration period on modelling
22 climate change impact on future runoff, Proc. IAHS, 371, 3-6, doi:10.5194/piahs-371-3-2015,
23 2015.
- 24 Heinrich, G. and Gobiet, A.: reclip:century 1 Research for Climate Protection: Century
25 Climate Simulations: Expected Climate Change and its Uncertainty in the Alpine Region,
26 ACRP final report reclip:century part D, Graz, Austria, 48 pp, 2011.
- 27 Jacob, D., Petersen, J., Eggert, B., Alias, A., Christensen, O. B., Bouwer, L., Braun, A.,
28 Colette, A., Déqué, M., Georgievski, G., Georgopoulou, E., Gobiet, A., Menut, L., Nikulin,
29 G., Haensler, A., Hempelmann, N., Jones, C., Keuler, K., Kovats, S., Kröner, N., Kotlarski,
30 S., Kriegsmann, A., Martin, E., Meijgaard, E., Moseley, C., Pfeifer, S., Preuschmann, S.,
31 Radermacher, C., Radtke, K., Rechid, D., Rounsevell, M., Samuelsson, P., Somot, S.,

- 1 Soussana, J.-F., Teichmann, C., Valentini, R., Vautard, R., Weber, B. and Yiou, P.: EURO-
2 CORDEX: new high-resolution climate change projections for European impact research
3 Regional Environmental Change, Springer, Berlin, Heidelberg, Germany, 1-16, 2013.
- 4 Koffler, D., and Laaha, G.: lfstat: Calculation of Low Flow Statistics for daily stream flow
5 data. R package version 0.5. <http://CRAN.R-project.org/package=lfstat>, (last access: 20
6 November 2015), 2014.
- 7 Laaha, G., and Blöschl, G.: Seasonality indices for regionalizing low flows, *Hydrolog.*
8 *Process.*, 20, 3851–3878, doi: 10.1002/hyp.6161, 2006.
- 9 Laaha, G. and Blöschl, G.: A national low flow estimation procedure for Austria,
10 *Hydrological Sciences Journal*, 52(4), 625–644, 2007.
- 11 Laaha, G., Parajka, J., Viglione, A., Koffler, D., Haslinger, K., Schöner, W., Zehetgruber, J.,
12 and Blöschl, G.: A three-pillar approach to assess climate impacts on low flows, submitted to
13 HESSD, 2015.
- 14 Lafaysse, M., Hingray, B., Mezghani, A., Gailhard, J., and Terray, L.: Internal variability and
15 model uncertainty components in future hydrometeorological projections: The Alpine
16 Durance basin, *Water Resour. Res.*, 50, 3317–3341, doi:10.1002/ 2013WR014897, 2014.
- 17 Loibl, W., Formayer, H., Schöner, W., Truhetz, H., Anders, I., Gobiet, A., Heinrich, G.,
18 Köstl, M., Nadeem, I., Peters Anders, J., Schicker, I., Suklitsch, M., and Züger, H.:
19 reclip:century 1 Research for Climate Protection: Century Climate Simulations: Models, Data
20 and GHG Scenarios, Simulations, ACRP final report reclip:century part A, Vienna, 22 pp,
21 2011.
- 22 Merz, R., Parajka, J., and Blöschl, G.: Time stability of catchment model parameters:
23 Implications for climate impact analyses, *Water Resour. Res.*, 47, W02531,
24 doi:10.1029/2010WR009505, 2011.
- 25 Moss, R. H., Edmonds, J. A., Hibbard, K. A., Manning, M. R., Rose, S. K., van Vuuren, D.
26 P., Carter, T. R., Emori, S., Kainuma, M., Kram, T., Meehl, G. A., Mitchell, J. F. B.,
27 Nakicenovic, N., Riahi, K., Smith, S. J., Stouffer, R. J., Thomson, A. M., Weyant, J. P., and
28 Wilbanks, T. J.: The next generation of scenarios for climate change research and assessment,
29 *Nature*, 463, 747-756, 2010.

- 1 Najafi, M.R., Moradkhani, H., and Jung, I.W.: Assessing the uncertainties of hydrologic
2 model selection in climate change impact studies, *Hydrol. Process.* 25, 2814–2826, DOI:
3 10.1002/hyp.8043, 2011.
- 4 Nakicenovic, N., Alcamo, J., Davis, G., de Vries, B., Fenmann, J., Gaffin, S., Gregory, K.,
5 Grübler, A., Jung, T. Y., Kram, T., La Rovere, E. L., Michaelis, L., Mori, S., Morita, T.,
6 Pepper, W., Pitcher, H., Price, L., Raihi, K., Roehrl, A., Rogner, H.-H., Sankovski, A.,
7 Schlesinger, M., Shukla, P., Smith, S., Swart, R., van Rooijen, S., Victor, N. and Dadi, Z.:
8 IPCC Special Report on Emissions Scenarios. Cambridge University Press: Cambridge,
9 United Kingdom and New York, 599 pp, 2000.
- 10 Parajka, J., Merz, R., and Blöschl, G.: Uncertainty and multiple objective calibration in
11 regional water balance modelling: case study in 320 Austrian catchments, *Hydrol. Process.*,
12 21, 435–446, doi:10.1002/hyp.6253, 2007.
- 13 Parajka, J., and Blöschl, G.: The value of MODIS snow cover data in validating and
14 calibrating conceptual hydrologic models, *Journal of Hydrology*, 358, 240–258, 2008.
- 15 Parajka, J., Merz, R., Skøien, J.O., and Viglione, A.: The role of station density for predicting
16 daily runoff by TOP-KRIGING interpolation in Austria, *Journal of Hydrology and*
17 *Hydromechanics*, 63, 1 - 7, 2015, doi: 10.1515/johh-2015-0024.
- 18 Prein, A. F., Gobiet, A. and Truhetz, H.: Analysis of uncertainty in large scale climate change
19 projections over Europe, *Met. Zet.*, 20 (4), 383-395, 2011.
- 20 Prudhomme, Ch., and Davies, H.: Assessing uncertainties in climate change impact analyses
21 on the river flow regimes in the UK. Part 2: future climate, *Climatic Change*, 93, 177–195,
22 DOI 10.1007/s10584-008-9464-3, 2009.
- 23 Skoien, J.O., Blöschl, G., Laaha, G., Pebesma, E., Parajka, J., and Viglione, A.: rtop: An R
24 package for interpolation of data with a variable spatial support, with an example from river
25 networks, *Computers & Geosciences*, Volume 67, Pages 180-190,
26 <http://dx.doi.org/10.1016/j.cageo.2014.02.009>, 2014.
- 27 Van der Linden, P., and Mitchell, J. F. B. (eds.): ENSEMBLES: Climate Change and its
28 Impacts: Summary of research and results from the ENSEMBLES project, Met Office Hadley
29 Centre, Exeter, United Kingdom, 160pp, 2009.

- 1 Van Loon, A. F. and Van Lanen, H. A. J.: A process-based typology of hydrological drought,
2 Hydrol. Earth Syst. Sci., 16, 1915–1946, doi:10.5194/hess-16-1915-2012, 2012.
- 3 Van Loon, A.F., Ploum, S.W., Parajka, J., Fleig, A.K., Garnier, E., Laaha, G., and Van Lanen,
4 H.A.J.: Hydrological drought types in cold climates: quantitative analysis of causing factors
5 and qualitative survey of impacts, Hydrol. Earth Syst. Sci., 19, 1993–2016, 2015.
- 6 Vidal, J.-P., Hingray, B., Magand, C., Sauquet, E., and Ducharne, A.: Hierarchy of climate
7 and hydrological uncertainties in transient low flow projections, Hydrol. Earth Syst. Sci.
8 Discuss., 12, 12649-12701, doi:10.5194/hessd-12-12649-2015, 2015.
- 9 Viglione, A., Parajka, J., Rogger, M., Salinas, J.L., Laaha, G., Sivapalan, M., and Blöschl, G.:
10 Comparative assessment of predictions in ungauged basins; Part 3: Runoff signatures in
11 Austria. Hydrology and Earth System Sciences, 17, 2263-2279, 2013.
- 12 Viglione, A., and Parajka, J.: TUWmodel: Lumped Hydrological Model for Education
13 Purposes. R package version 0.1-4. <http://CRAN.R-project.org/package=TUWmodel>, (last
14 access: 20 November 2015), 2014.
- 15 von Storch, H., and Zwiers, F.W.: Statistical analysis in climate research, Cambridge
16 University press, ISBN 0 521 45071 3, 484pp, 1999.
- 17 Zessner M.: Transboundary pollution and water quality policies in Austria, Water Science &
18 Technology, 58.10, 2008.
- 19
- 20
- 21
- 22

1

2 Table 1. TUWmodel parameters. Calibration range is given for parameters calibrated by an
 3 automatic routine. Parameters with fixed value are not calibrated.

Model parameter	Definition	Model component	Calibration range
SCF	Snow correction factor (dimensionless)	Snow	1.0-1.5
DDF	Degree-day factor (mm/ $^{\circ}$ C day)	Snow	0.0-5.0
T _R	Threshold temperature for rain ($^{\circ}$ C)	Snow	2.0
T _S	Threshold temperature for snow ($^{\circ}$ C)	Snow	0.0
T _M	Melt temperature ($^{\circ}$ C)	Snow	-1.0-3.0
LP/FC	Ratio of limit for potential evapotranspiration and FC (dimensionless)	Soil	0.0-1.0
FC	Maximum soil moisture storage (mm)	Soil	0.0-600.0
BETA	Nonlinearity parameter of runoff generation (dimensionless)	Soil	0.0-20.0
K ₀	Storage coefficient of additional outlet (days)	Runoff	0.0-2.0
K ₁	Fast storage coefficient (days)	Runoff	2.0-30.0
K ₂	Slow storage coefficient (days)	Runoff	30.0-250.
C _P	Percolation rate (mm/d)	Runoff	0.0-8.0
C _R	Free routing coefficient (days ² /mm)	Runoff	25.0
LS _{UZ}	Storage capacity threshold (mm)	Runoff	1.0-100.0
Bmax	Routing parameter (days)	Runoff	10.0

4

5

6

1

2 Table 2. Summary of seasonal and annual changes in the mean basin precipitation and air
 3 temperature as simulated by four selected RCM runs. The first value and values in the
 4 brackets are the median and range (min/max) of differences between the future (2021-2050)
 5 and reference (1978-2007) periods in 262 basins. Winter and summer seasons are defined as
 6 December-May and June-November, respectively.

Delta change	WEGC*	ZAMG**	AIT***	HADCM3	ZAMG ECHAM5
	ECHAM5 A1B	ECHAM5		A1B	B1
		A2			
Air temperature					
winter (°C)	+1.5 (0.9/1.7)	+0.7 (-1.1/2.1)	+1.3 (0.8/1.5)	+1.0 (-0.8/2.5)	
Air temperature					
summer (°C)	+1.2 (0.8/1.7)	+0.9 (-0.1/2.2)	+2.1 (1.4/2.4)	+1.3 (0.4/2.5)	
Air temperature					
year (°C)	+1.3 (0.9/1.5)	+0.8 (-0.4/2.2)	+1.7 (1.2/1.9)	+1.2 (0.0/2.5)	
Precipitation					
winter (%)	+8.2 (-0.7/16.2)	-1.5 (-5.8/6.4)	+1.3 (-9.6/6.8)	0.0 (-8.5/3.3)	
Precipitation					
summer (%)	-6.2 (-9.9/3.7)	+0.2 (-8.9/5.7)	-5.0 (-13.5/0.2)	-2.3 (-6.3/2.5)	
Precipitation					
year (%)	+0.9 (-4.6/8.7)	-0.9 (-4.1/3.4)	-2.0 (-9.3/1.8)	-1.2 (-5.5/2.8)	

7 *WEGC= Wegener Center for Climate and Global Change

8 **ZAMG= Zentralanstalt für Meteorologie und Geodynamik

9 ***AIT= Austrian Institute of Technology

10

11

1

2 Figure captions:

3 Figure 1. Topography of Austria and location of 262 river flow gauges. Colour and symbol
4 size of the gauges represent seasonality of low flows SI and its strength (r) in the period 1976-
5 2008, respectively. The SI and its strength are estimated by R lfstat package (Koffler and
6 Laaha, 2014).

7 Figure 2. Mean annual air temperature (MAT, top), precipitation (MAP, middle) and runoff
8 (MAR, bottom) for basins with summer (yellow/red) and winter (blue) low-flow minima
9 (Fig.1). Thin lines represent the median of mean annual values of MAT, MAP and MAR.
10 Thick lines indicate the average for each of the three periods: 1976-86, 1987-97 and 1998-08.
11 Scatter (i.e. 75% and 25%- percentiles) indicates the variability between the basins.

12 Figure 3. Runoff model efficiency (Z_Q) for different calibration weights w_Q in three different
13 calibration periods. Lines represent the medians, scatter (i.e. 75%-25% percentiles) shows the
14 Z_Q variability over basins with dominant winter (blue) and summer (orange) low-flow regime.

15 Figure 4. Difference between simulated and observed low-flow characteristics (top panels
16 low-flow quantile Q_{95} , bottom panels seasonality index SI) for different calibration variants
17 (w_Q) and calibration periods. Lines represent the median, scatter (i.e. 75%-25% percentiles)
18 show the variability over basins with dominant winter (blue) and summer (orange) low flow
19 regime. The differences are estimated between model simulations and observations in the
20 entire reference period 1976-2008.

21 Figure 5. Comparison of observed (blue) and simulated (red) flow for
22 Hoheneich/Braunaubach, 291.5 km^2). Thick lines show flows below low-flow quantile Q_{95} .
23 Model simulations are based on calibration variant $w_Q=0.5$ in the period 1998-2008. The
24 relative difference between Q_{95} estimated from simulated and observed flows is 8%.

25 Figure 6. Uncertainty of Q_{95} model simulations estimated from 11 calibration variants
26 calibrated in the same calibration period (right panels, top - calibration period 1976-1986,
27 bottom - calibration period 1998-2008) and from three calibration periods calibrated by the
28 same calibration variant (left panels, top $w_Q=0.5$, bottom $w_Q=0.0$). The uncertainty is
29 expressed as the range of relative differences (%) between simulated and observed Q_{95}
30 obtained by particular calibration variants in the period 1976-2008. Colour patterns in the

1 background show the interpolated ranges by using top-kriging method (Skoien et al., 2014,
2 Parajka et al., 2015).

3 Figure 7. Uncertainty of simulations of low-flow seasonality (*SI*) estimated from 11
4 calibration variants calibrated in the same calibration period (right panels, top - calibration
5 period 1976-1986, bottom - calibration period 1998-2008) and from three calibration periods
6 calibrated by the same calibration variant (left panels, top $w_Q=0.5$, bottom $w_Q=0.0$). The
7 uncertainty is expressed as the range of differences (days) between simulated and observed *SI*
8 in the period 1976-2008. Colour patterns in the background show the interpolated ranges by
9 using top-kriging.

10 Figure 8. Projections of low flows for selected climate scenarios and calibration variants. Line
11 represents the medians, scatter (i.e. 75%-25% percentiles) shows the variability over 262
12 basins. Top and bottom panels show projected changes of low-flow quantiles Q_{95} and
13 seasonality index *SI* in basins with winter (blue) and summer (orange) low-flow regimes,
14 respectively. Projections indicate future changes with respect to the reference period 1976-
15 2008. Calibration variants are calibrated in the period 1998-2008.

16 Figure 9. Projections of low-flow quantiles Q_{95} changes for four climate scenarios in 262
17 Austrian basins. Model simulations are based on variant $w_Q=0.5$ calibrated in the period 1998-
18 2008. Colour patterns in the background show the interpolated projections by using top-
19 kriging.

20 Figure 10. Projections of changes in low-flow seasonality (*SI*) for four climate scenarios in
21 262 Austrian basins. Model simulations are based on variant $w_Q=0.5$ calibrated in the period
22 1998-2008. Colour patterns in the background show the interpolated projections by using top-
23 kriging.

24 Figure 11. Uncertainty of Q_{95} model projections of low flows for four different climate
25 scenarios. The uncertainty is expressed as the range of relative differences (%) between Q_{95}
26 simulated in the future and reference period obtained for 11 calibration variants calibrated in
27 three calibration periods. Colour patterns in the background show the interpolated ranges by
28 using top-kriging.

29 Figure 12. Uncertainty of model projections of low-flow seasonality for four different climate
30 scenarios. The uncertainty is expressed as the range of relative differences (%) between
31 seasonality occurrence (*SI*) simulated in the future and reference period obtained for 11

1 calibration variants calibrated in three calibration periods. Colour patterns in the background
2 show the interpolated ranges by using top-kriging.

3 Figure 13. Total uncertainty of model projections of low flows for four different climate
4 scenarios, 11 calibration variants and three calibration periods. The uncertainty is expressed
5 as the range of Q_{95} (left panel) and seasonality (right panel) of differences between model
6 simulations in the future and reference periods. Bottom panels show the ratio between the
7 range of climate projections to the range of differences in the reference period. Colour
8 patterns in the background show the interpolated ranges by using top-kriging.

9 Figure 14. Relationship between the uncertainty ratio between calibration and projection
10 uncertainty and basin area (left panels), mean basin elevation (middle panels) and aridity
11 index (right panels). Top and bottom panels show the uncertainty ratio for the low-flow
12 quantile (Q_{95}) and seasonality index (SI), respectively. Basins with winter low-flow
13 seasonality are plotted in blue, basins with summer low-flow seasonality are in yellow.

14 Figure 15. Relative contribution of the three variance components (i.e. climate scenario,
15 calibration decade and objective function) to the overall uncertainty of future low flow
16 projection in basins with winter (left panel) and summer (right panel) low-flow regime. The
17 boxes and whiskers show 25%- and 75%- percentiles and 5%- and 95%- percentiles of the
18 uncertainty contributions in 130 (summer low-flow regime) and 132 (winter low-flow regime)
19 basins, respectively.

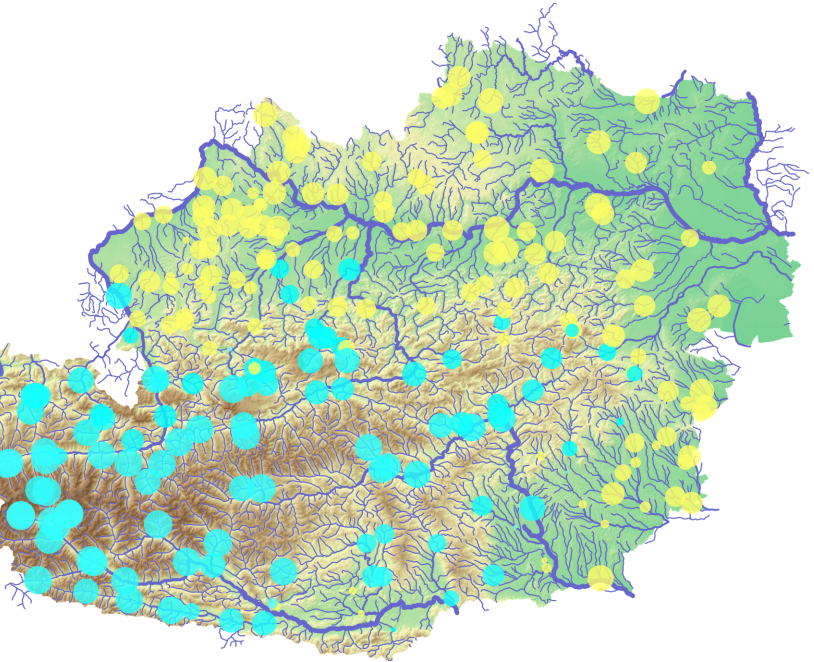
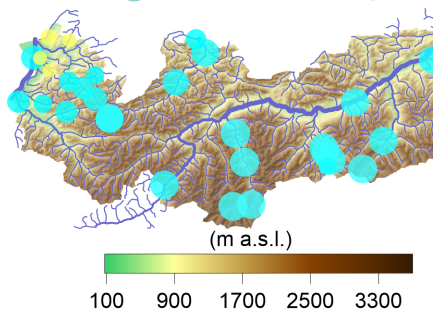
strength of seasonality

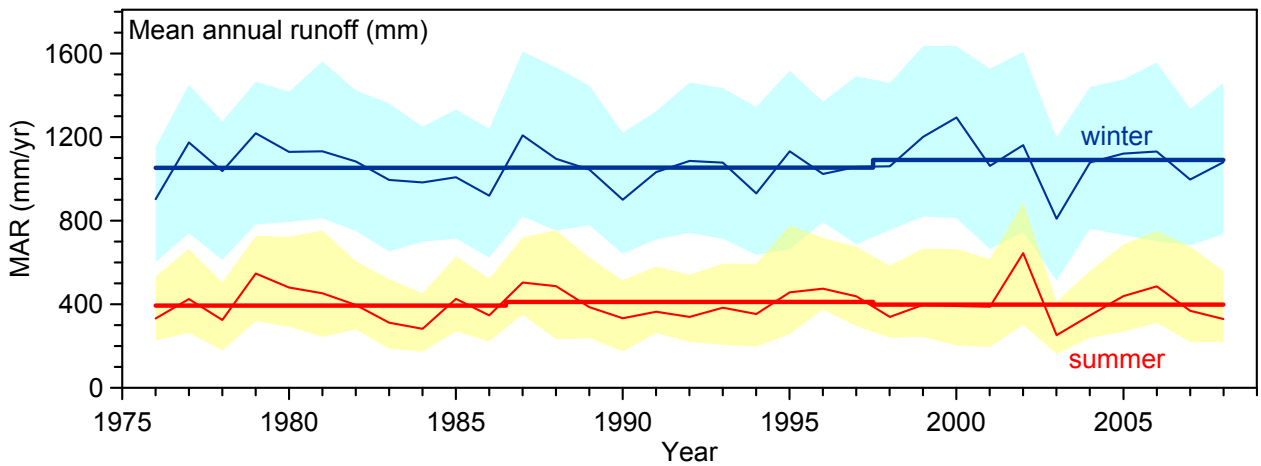
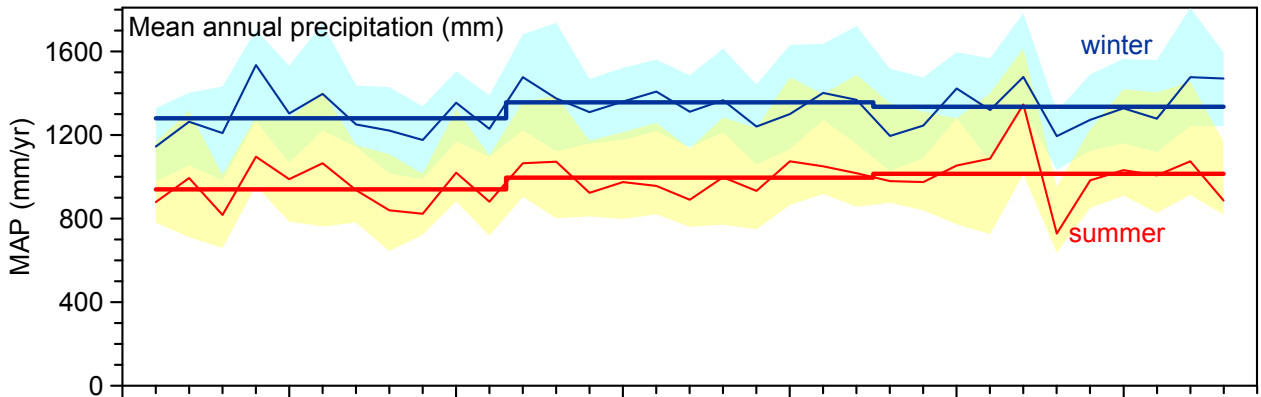
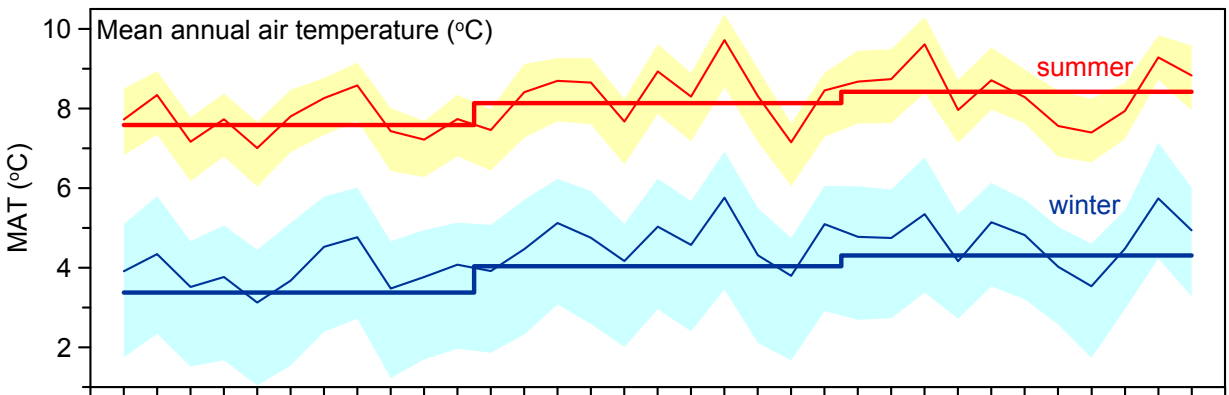
• low

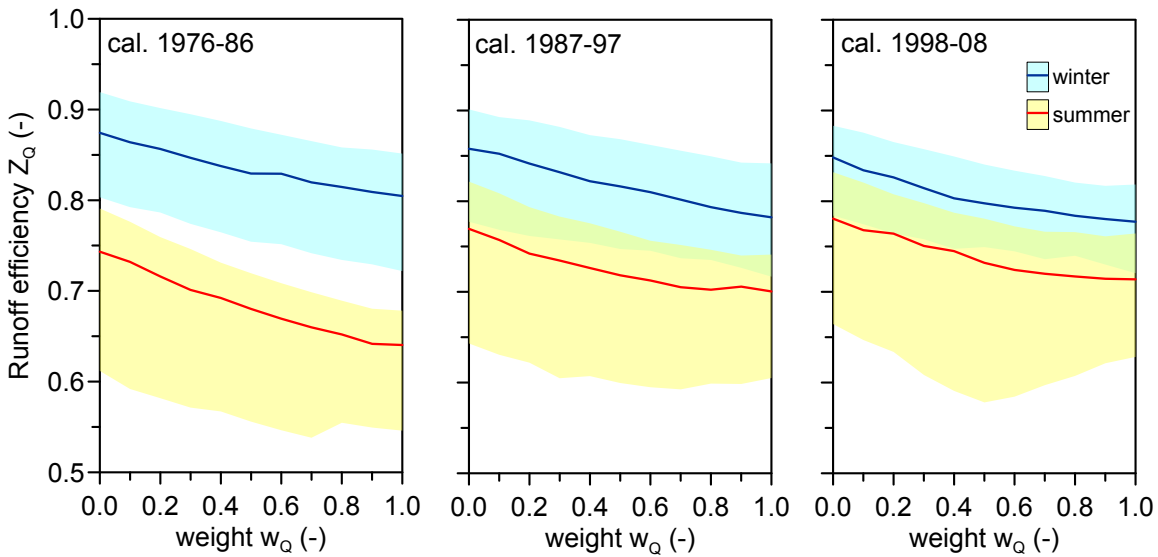
● large

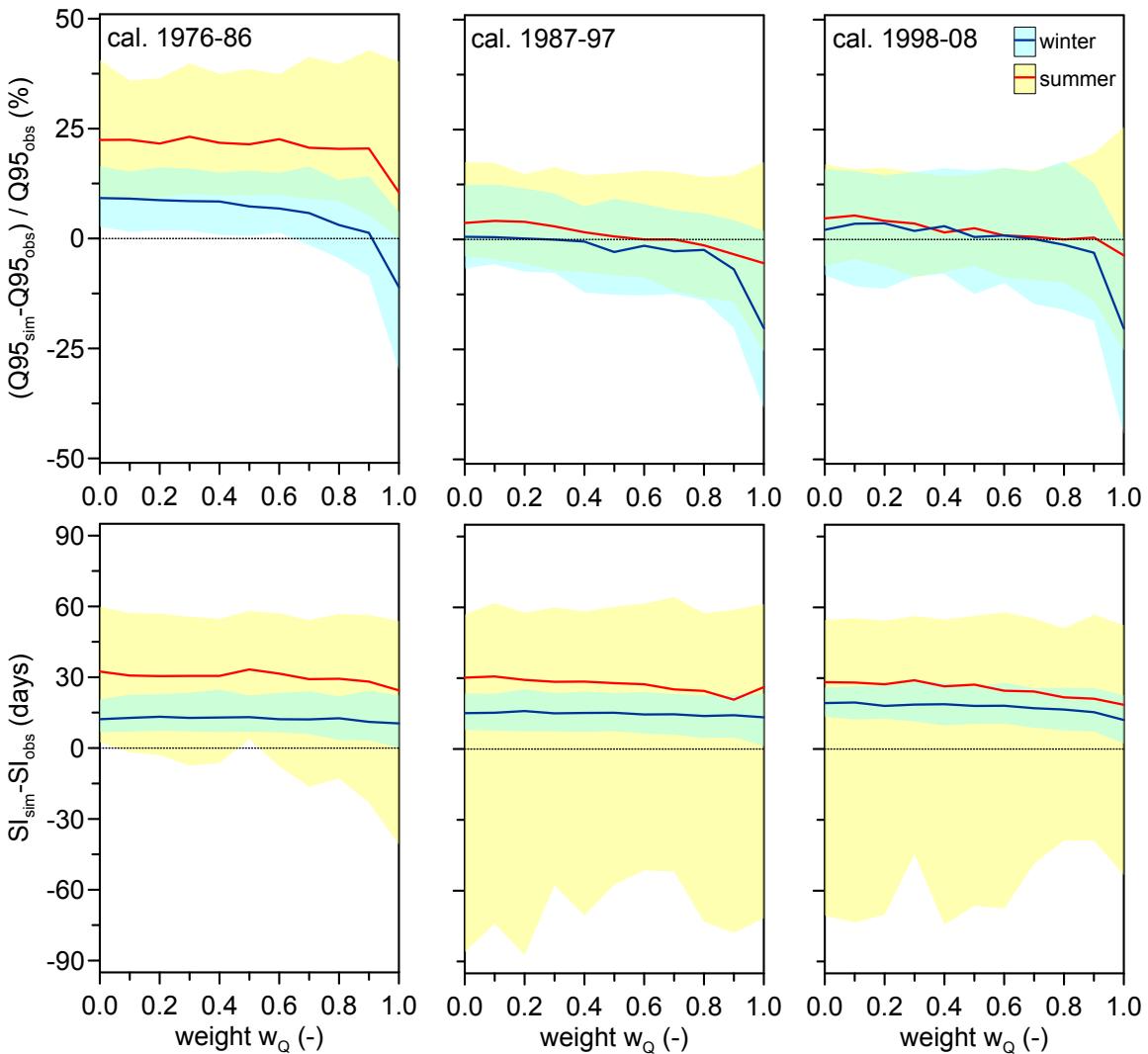
○ summer low-flow regime

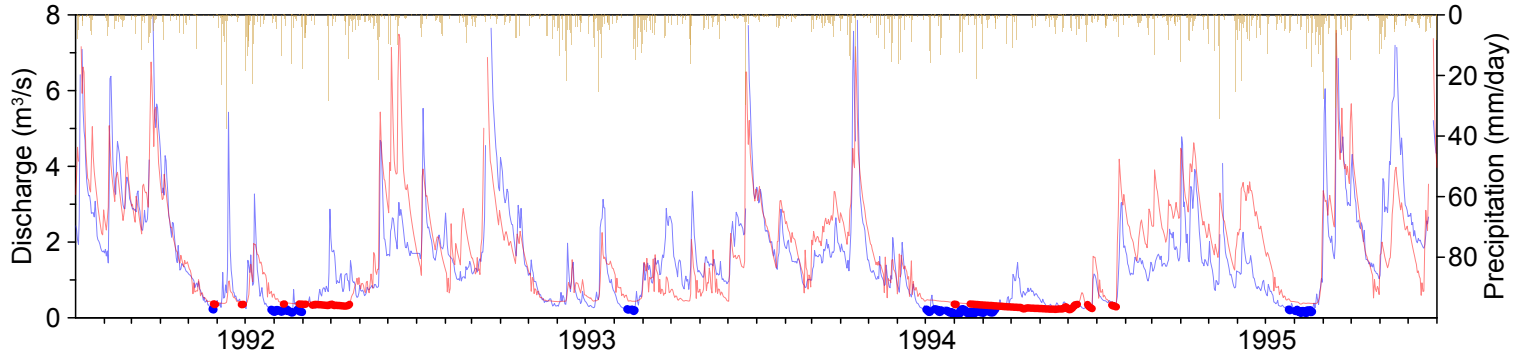
○ winter low-flow regime



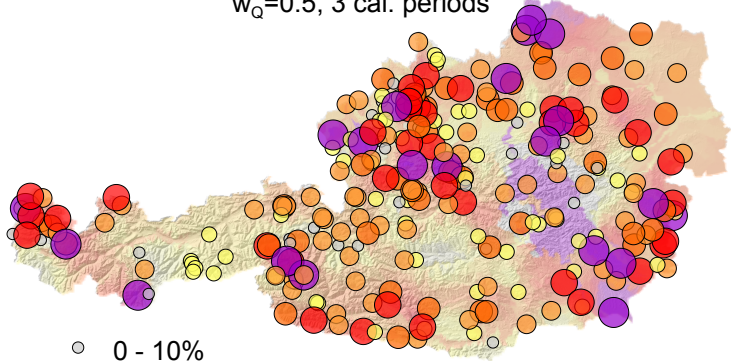




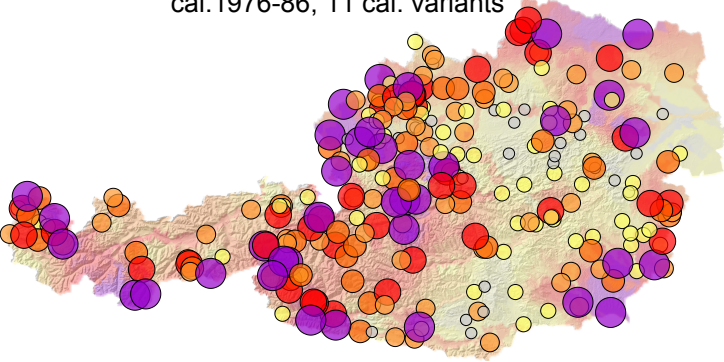




$w_Q=0.5$, 3 cal. periods

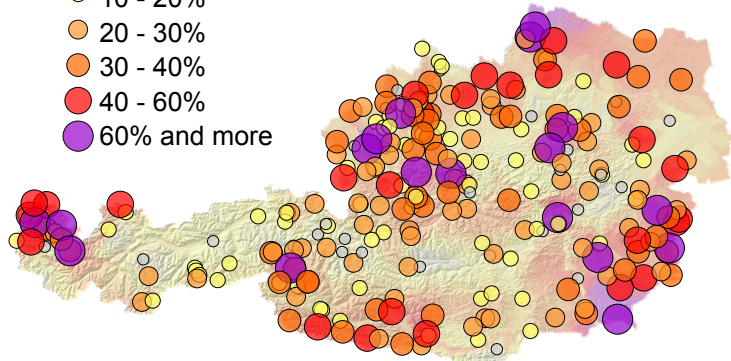


cal.1976-86, 11 cal. variants

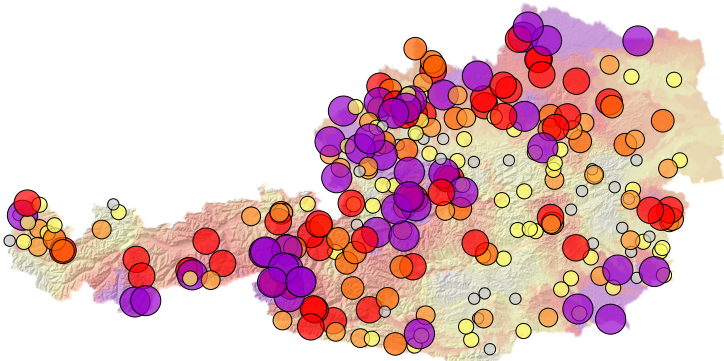


- 0 - 10%
- 10 - 20%
- 20 - 30%
- 30 - 40%
- 40 - 60%
- 60% and more

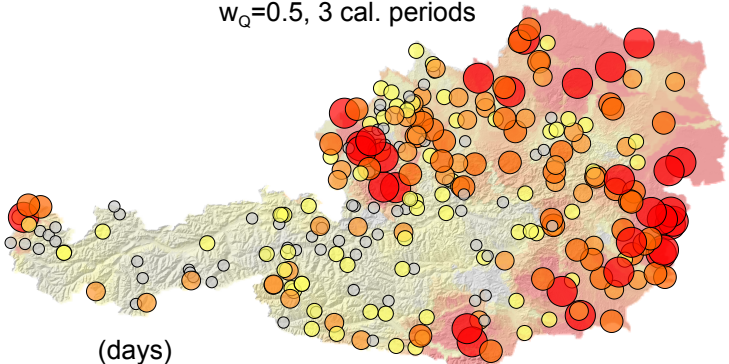
$w_Q=0.0$, 3 cal. periods



cal.1998-08, 11 cal. variants



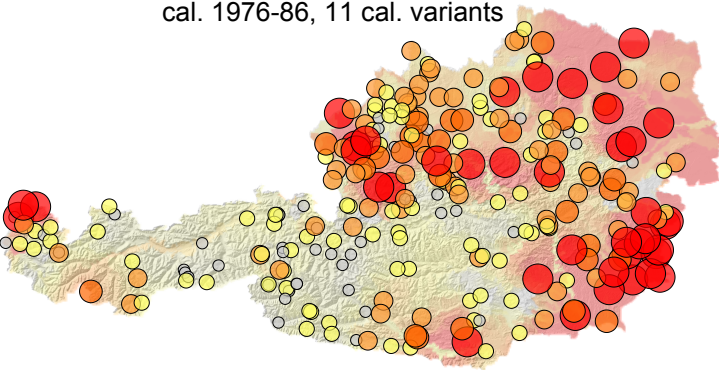
$w_Q=0.5$, 3 cal. periods



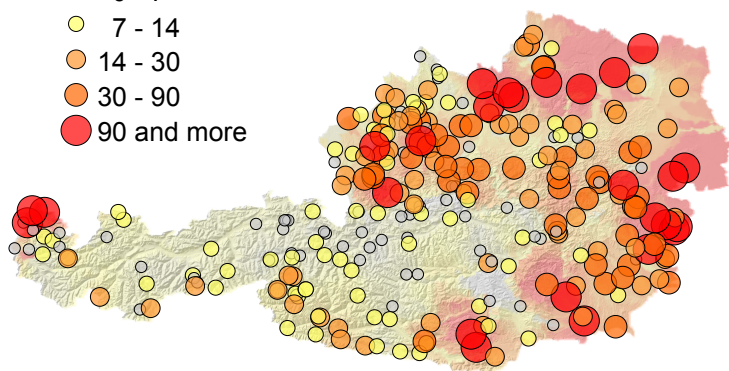
(days)

- 0 - 7
- 7 - 14
- 14 - 30
- ▲ 30 - 90
- ◆ 90 and more

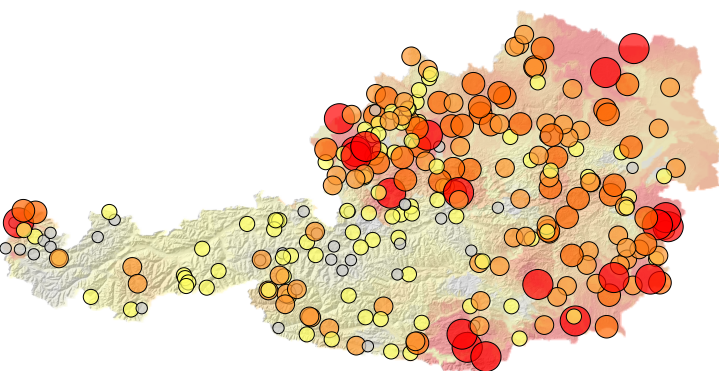
cal. 1976-86, 11 cal. variants

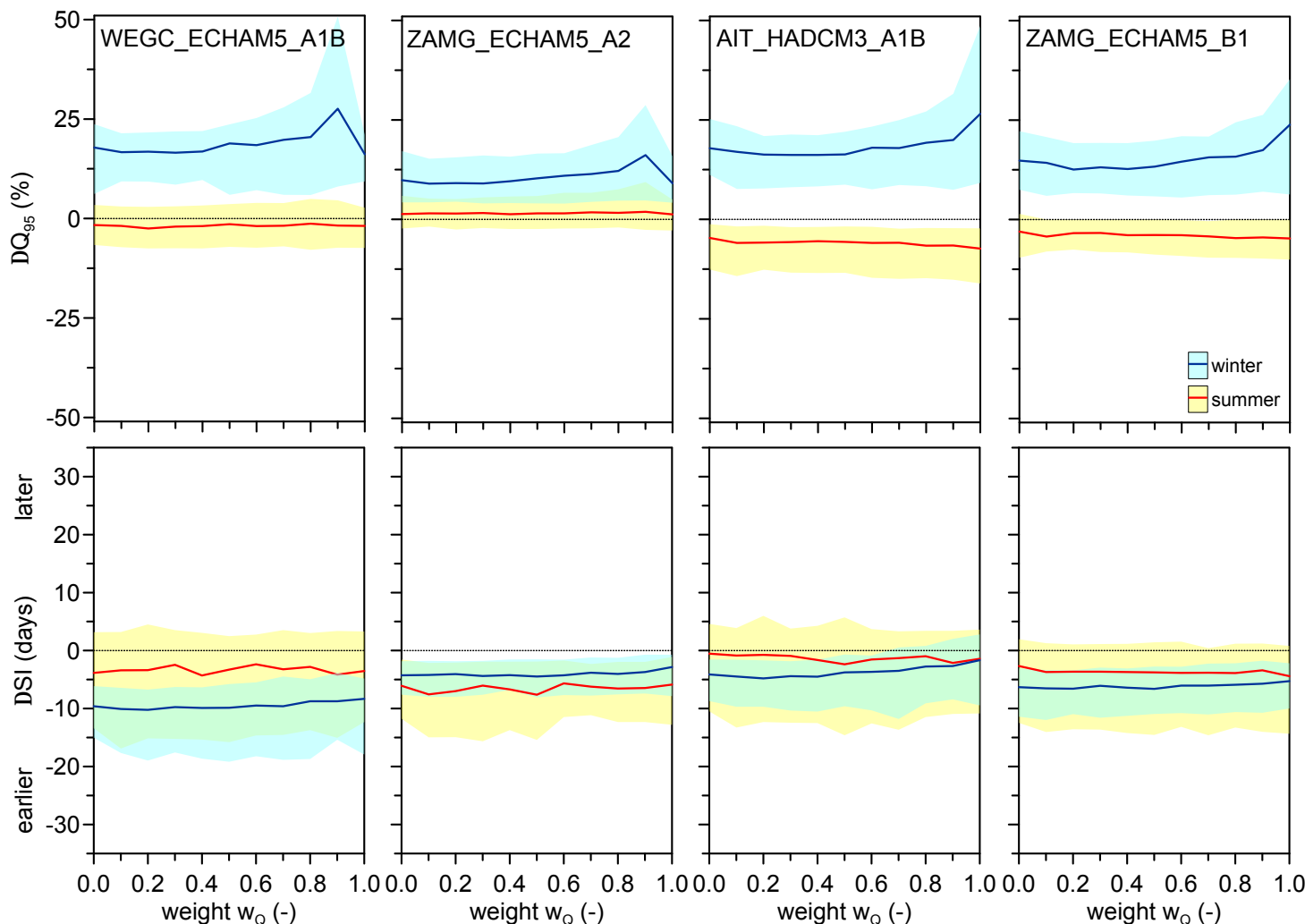


$w_Q=0.0$, 3 cal. periods

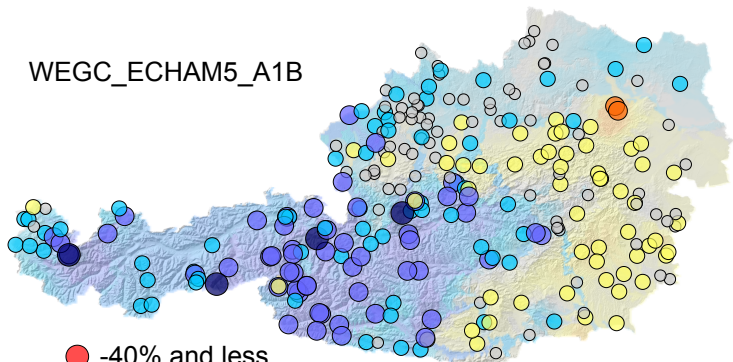


cal. 1998-08, 11 cal. variants

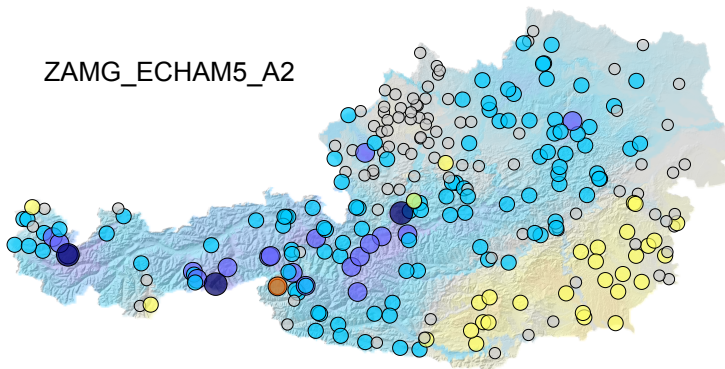




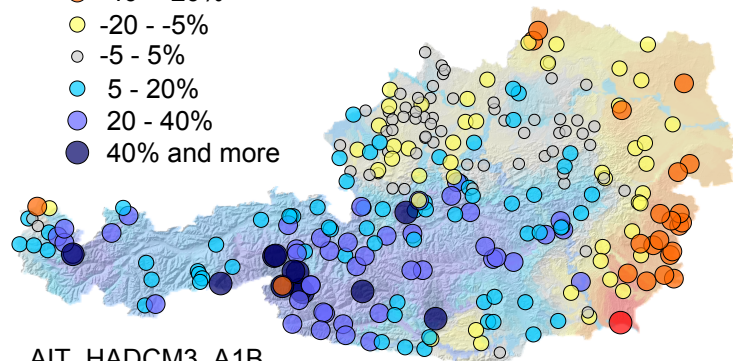
WEGC_ECHAM5_A1B



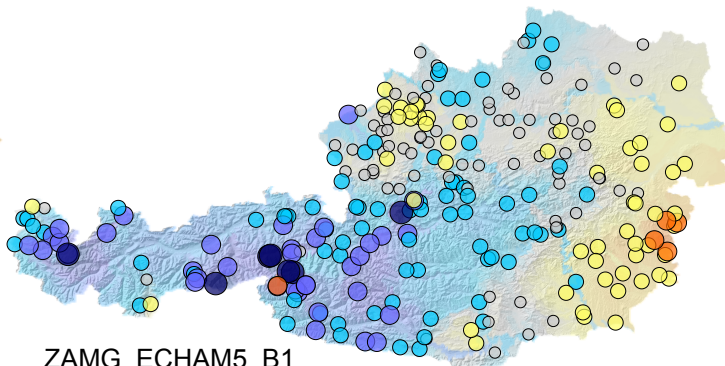
ZAMG_ECHAM5_A2



AIT_HADCM3_A1B

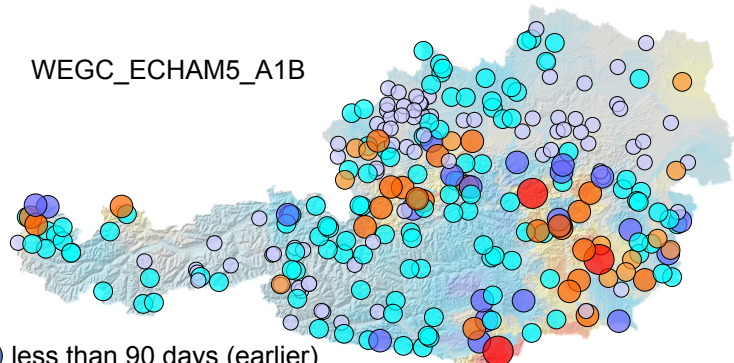


ZAMG_ECHAM5_B1

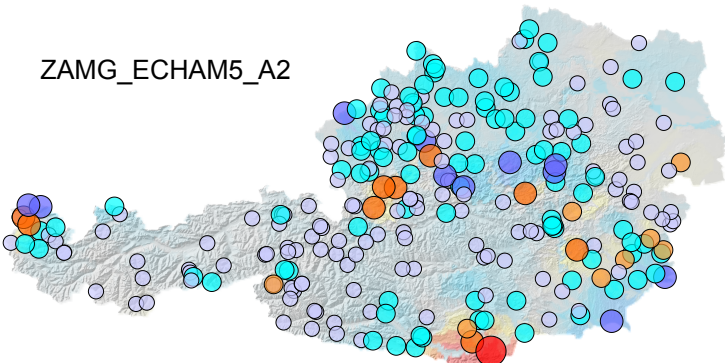


- -40% and less
- -40 - -20%
- -20 - -5%
- -5 - 5%
- 5 - 20%
- 20 - 40%
- 40% and more

WEGC_ECHAM5_A1B

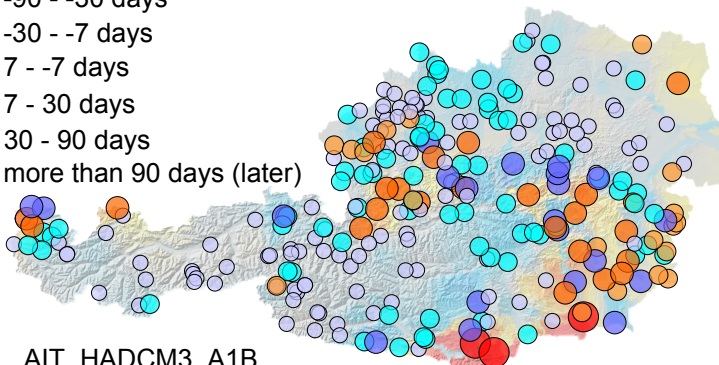


ZAMG_ECHAM5_A2

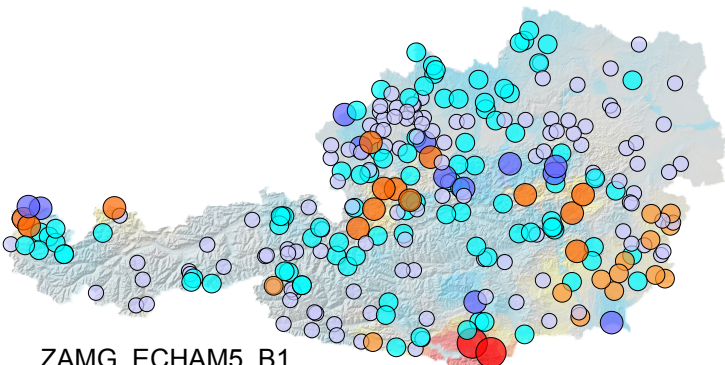


- less than 90 days (earlier)
- 90 - -30 days
- 30 - -7 days
- 7 - -7 days
- 7 - 30 days
- 30 - 90 days
- more than 90 days (later)

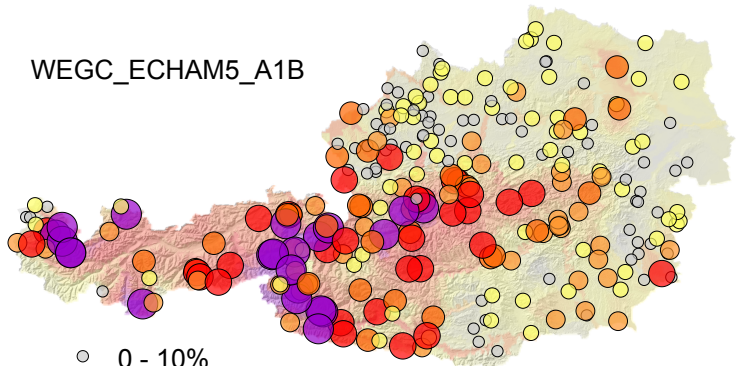
AIT_HADCM3_A1B



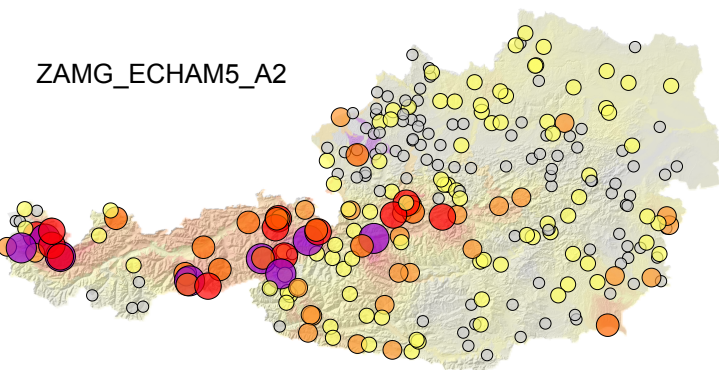
ZAMG_ECHAM5_B1



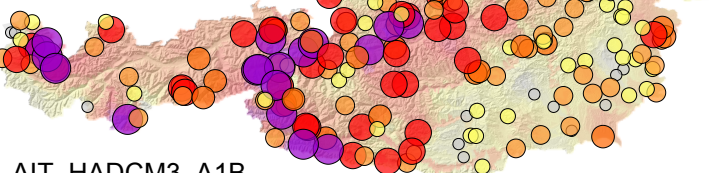
WEGC_ECHAM5_A1B



ZAMG_ECHAM5_A2

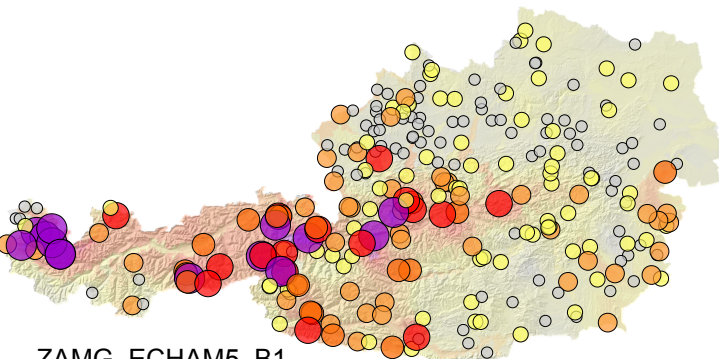


• 0 - 10%
• 10 - 20%
• 20 - 30%
• 30 - 40%
• 40 - 60%
• 60% and more

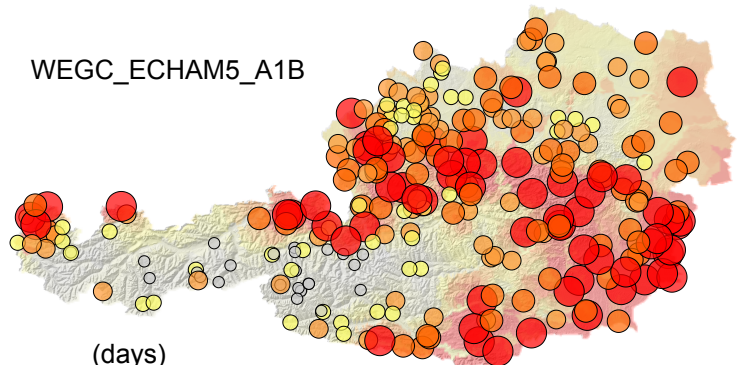


AIT_HADCM3_A1B

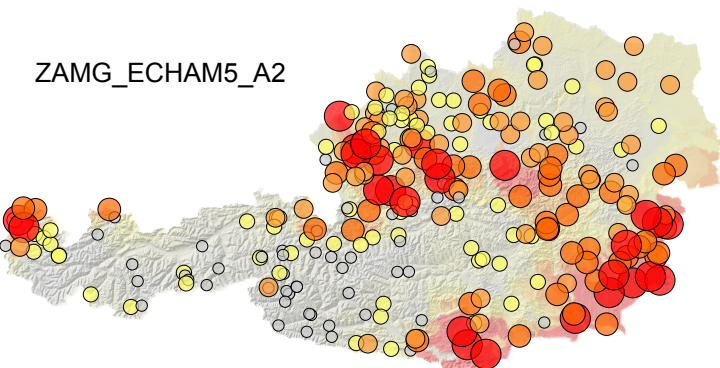
ZAMG_ECHAM5_B1



WEGC_ECHAM5_A1B

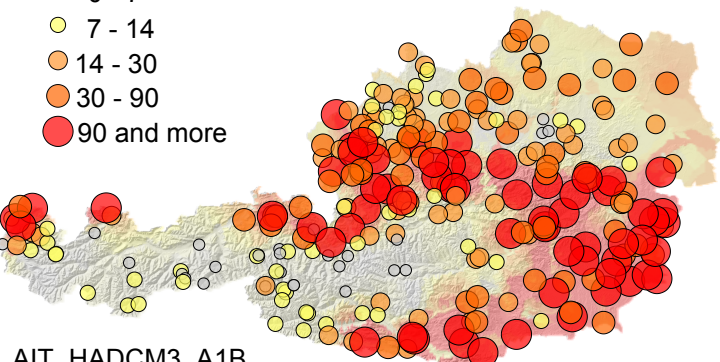


ZAMG_ECHAM5_A2



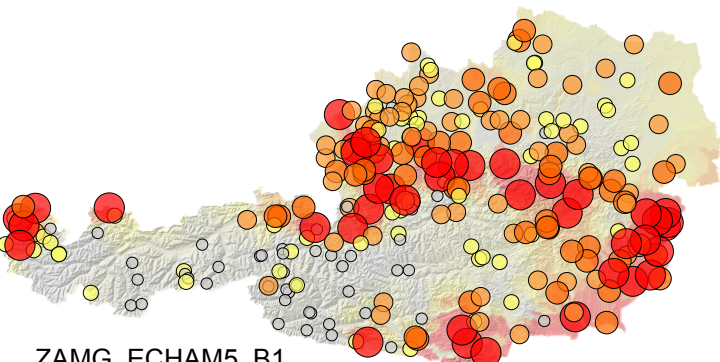
(days)

- 0 - 7
- 7 - 14
- 14 - 30
- 30 - 90
- 90 and more

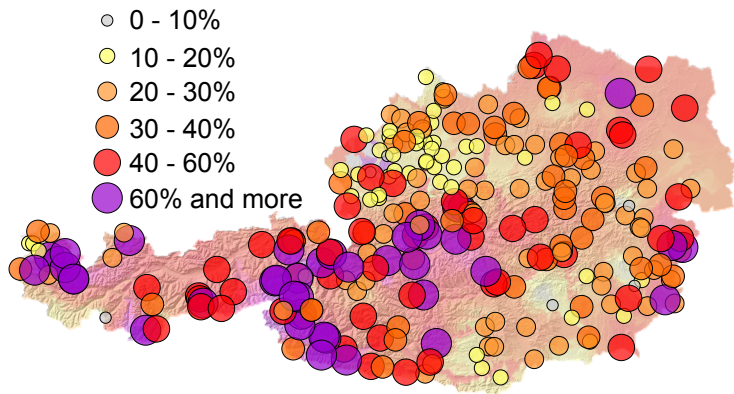


AIT_HADCM3_A1B

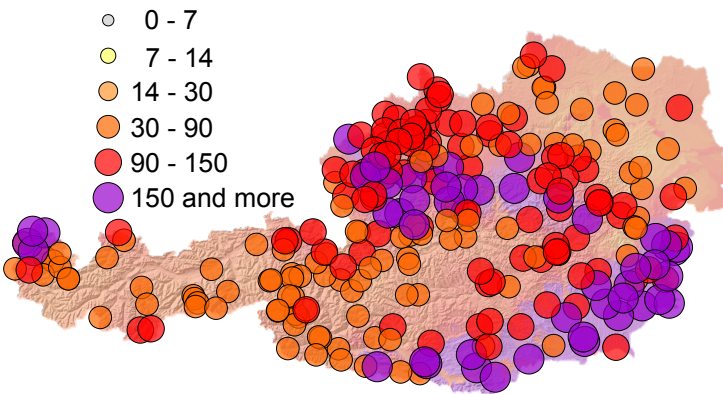
ZAMG_ECHAM5_B1



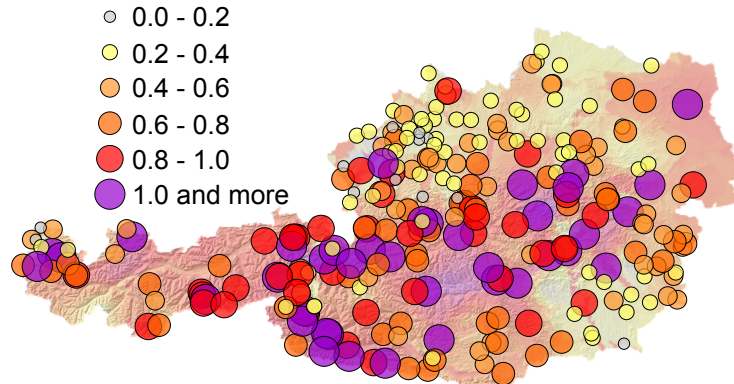
Total range: Q₉₅ projections (%)



Total range: SI projections (days)



Range projections / Range calibrations



Range projections / Range calibrations

